

Technische Universität Berlin

Big Data Engineering (DAMS)

Fakultät IV

Ernst-Reuter-Platz 7

10587 Berlin

<https://www.tu.berlin/dams>



Bachelor Thesis

Learned Quantization Schemes for Data-centric ML Pipelines

Anuun Chinbat

Matriculation Number: 0463111

20.01.2025

Supervised by
Prof. Dr. Matthias Boehm
M.Sc. Sebastian Baunsgaard

Eigenständigkeitserklärung

Hiermit versichere ich, dass ich die vorliegende Arbeit eigenständig ohne Hilfe Dritter und ausschließlich unter Verwendung der aufgeführten Quellen und Hilfsmittel angefertigt habe. Alle Stellen die den benutzten Quellen und Hilfsmitteln unverändert oder sinngemäß entnommen sind, habe ich als solche kenntlich gemacht.

Sofern generische KI-Tools verwendet wurden, habe ich Produktnamen, Hersteller, die jeweils verwendete Softwareversion und die jeweiligen Einsatzzwecke (z.B. sprachliche Überprüfung und Verbesserung der Texte, systematische Recherche) benannt. Ich verantworte die Auswahl, die Übernahme und sämtliche Ergebnisse des von mir verwendeten KI-generierten Outputs vollumfänglich selbst.

Die Satzung zur Sicherung guter wissenschaftlicher Praxis an der TU Berlin vom 8. März 2017. https://www.static.tu.berlin/fileadmin/www/10000060/FSC/Promotion__Habilitation/Dokumente/Grundsätze_gute_wissenschaftliche_Praxis_2017.pdf habe ich zur Kenntnis genommen. Ich erkläre weiterhin, dass ich die Arbeit in gleicher oder ähnlicher Form noch keiner anderen Prüfungsbehörde vorgelegt habe.

Berlin, 20.01.2024

.....

Abstract

Machine learning (ML) models are notoriously resource-intensive. Given their widespread application on end-user devices, the need to reduce the memory and computing requirements of such models is becoming ever more pressing. Interestingly, the very redundancy that contributes to the inefficient nature of predictive models, offers the remedy to the issue of resource-intensiveness by creating opportunities for exploitation. One way to exploit the redundancy of Neural Networks (NNs) is to *quantize* them — to approximate their full-precision representations with lower-bit-width floating point representations. Among the various quantization approaches, *learned quantization* presents itself as a promising research area with room for contribution, considering the vast landscape of opportunities for ML models to autonomously learn their optimal quantization strategies. Hence, this work introduces two techniques for learned quantization, achieving effective model compression without incurring significant accuracy degradation. The first technique involves custom regularization terms that directly take into account quantization goals, the second novel approach incorporates a custom scaling factor gradient calculation that utilizes the gradient of the parameters that are being quantized. As a result, we achieve a memory usage reduction of up to 10 \times for the model weights trained on MNIST, CIFAR-10, and Imagenette, a simplified ImageNet dataset.

Zusammenfassung

Machine Learning (ML) Modelle sind dafür bekannt, äußerst ressourcenintensiv zu sein. Da sie immer häufiger auf Endgeräten zum Einsatz kommen, wird die Notwendigkeit, Speicher- und Rechenaufwand zu verringern, zunehmend dringlich. Interessanterweise liefert die Redundanz, die maßgeblich zur Ineffizienz von neuronalen Netzen (NNs) beiträgt, zugleich auch den Ansatzpunkt, um genau diese Ineffizienz zu verringern. Eine Möglichkeit, die Redundanz von NNs auszunutzen, ist die Quantisierung – also die Ersetzung ihrer Präzisionsdarstellungen durch Varianten mit geringerer Bit-Breite. Unter den verschiedenen Ansätzen der Quantisierung erweist sich *Learned Quantization*, oder auch erlernte Quantisierung, aufgrund des breiten Spektrums an Möglichkeiten, bei denen ML Modelle selbstständig optimale Quantisierungsstrategien erlernen können, als ein vielversprechendes Forschungsfeld mit Raum für neue Beiträge. In dieser Arbeit werden daher zwei Techniken der Learned Quantization vorgestellt, die eine effektive Modellkompression ermöglichen, ohne zu wesentlichen Einbußen bei der Genauigkeit zu führen. Die erste Technik verwendet speziell angepasste Regularisierungsterme, die die Ziele der Quantisierung direkt berücksichtigen. Der zweite, neuartige Ansatz integriert eine einzigartige Berechnung des Gradienten für den Skalierungsfaktor, der den Gradienten der zu quantisierenden Parameter nutzt. Mit diesen Methoden lässt sich der Speicherbedarf für die Modellparameter – trainiert auf MNIST, CIFAR-10 und Imagenette (einer vereinfachten Version von ImageNet) – um das bis zu Zehnfache reduzieren, ohne dass die Genauigkeit maßgeblich beeinträchtigt wird.

Contents

Abstract	vi
Zusammenfassung	viii
1 Introduction	1
2 Background	3
2.1 Fundamentals of Deep Learning	3
2.1.1 Dense and Convolutional Layers	3
2.1.2 Loss Functions and Regularization	6
2.1.3 Forward-Pass and Back-Propagation	6
2.2 Basics of Quantization	7
2.2.1 Purpose and Definition	7
2.2.2 Core Quantization Approaches	8
2.3 Learned Quantization	10
2.3.1 Trade-offs and Challenges	10
2.3.2 Common Methods	12
3 Learned Quantization Schemes	15
3.1 Nested Quantization Layer	15
3.1.1 Core Logic and Structure	15
3.1.2 Learned Scale Factor	16
3.2 Custom Loss Function Terms	18
3.2.1 Design and Integration	18
3.2.2 Loss Term Definitions	20
4 Experiments	23
4.1 Experimental Setup	23
4.2 Analysis of Nested Quantization Layers	24
4.2.1 Fully Connected Layers	24
4.2.2 Convolutional Layers	27
4.3 Analysis of Custom Loss Terms	32
4.3.1 Fully Connected Layers	32
4.3.2 Convolutional Layers	34
5 Related Work	39

6 Conclusions	43
Bibliography	45

1 Introduction

Modern life runs on ML models working tirelessly in the background every day. From unlocking one’s phone with Face ID in the morning to receiving a curated recommendation feed on Netflix in the evening — all is ML — but at what cost?

If we consider GPT-3 as an example [3], its 175 billion parameters need a whopping 700 GB of storage in total — 4 bytes for each parameter represented in single-precision floating-point format (FP32). This costliness of modern ML models has increased interest in the research area of *quantization of NNs* which aims to reduce model size by developing methods that directly or indirectly decrease the amount of memory needed to store parameters numbering in the millions or billions. Going back to the GPT-3 example, by directly converting its FP32 parameters to 8-bit integers (INT8), we can reduce its storage requirement from 700 to just 175 GB — a $4\times$ decrease.

Quantization, however, comes with its own trade-offs. While some studies claim that quantization may improve a model’s generalization abilities by introducing noise that acts as regularization [7], it is still commonly expected to result in reduced accuracy. To limit the impact of quantization, a subfield known as *learned quantization* has emerged, focusing on developing schemes that allow models to learn their own quantization parameters during training, while preserving accuracy.

Various approaches of learned quantization have already been proposed [11, 23, 47, 49], each employing unique quantization schemes, while overcoming the inherent issue of non-differentiability of rounding operations. However, most of these methods rely on a predefined bit width, including but not limited to binary quantization [7, 18, 39] or an arbitrary user-defined bit width [49], thereby lacking the ability to dynamically control the “intensity” of quantization during training.

The option to explore *how much* quantization can be achieved, rather than simply deciding if a model can be quantized under given constraints, offers a broader perspective on a model’s behavior under quantization. For example, one could experiment with the intensity of quantization to determine a bit width that suits their requirements or, when resources and time are very limited and achieving maximum quantization is not the main focus, apply — perhaps unintuitively — a *minimal amount of quantization* to achieve moderate but still valuable results without taking too much risk.

Therefore, in this thesis, we address the lack of a flexible approach to control quantization intensity during training by contributing the following:

- We provide a modular framework in Subsection 3.1.1 that can be easily integrated into a wide range of applications and layers with minimal adjustments, ensuring flexibility and usability.

1 Introduction

- In Subsection 3.1.2, we introduce a novel method that uses the gradient-to-parameter ratio to determine how much a parameter is adjusted relative to its value. With this ratio and a hyperparameter λ controlling quantization intensity, the model learns its quantizing scaling factors at various granularities.
- We investigate, in Section 3.2, a method for the model to learn its scaling factors through a regularization term that can be tuned via a hyperparameter, enabling further control over the “intensity” of quantization.
- To demonstrate the effectiveness of the above contributions, we provide experimental results in Chapter 4.

2 Background

This chapter provides the theoretical and contextual background necessary to understand the key concepts and methodologies that form the foundation of this thesis. The first section introduces the fundamentals of deep NNs, which serve as a basis for the discussion. The next section broadens the perspective by exploring the concept of quantization, followed by the final section that explains common techniques of *learned quantization*, as well as the trade-offs and challenges they present.

2.1 Fundamentals of Deep Learning

This section introduces the fundamental concepts of deep learning, beginning with the most basic NN architecture components in Subsection 2.1.1 and progressing to loss functions with regularization in Subsection 2.1.2. The concepts of the forward-pass and back-propagation will be explained in the last Subsection 2.1.3.

2.1.1 Dense and Convolutional Layers

NNs can be considered a mathematical abstraction inspired by the structure and function of biological neural systems. At their core, they process inputs, transform them through intermediate or *hidden layers* of computation, and produce outputs. These hidden layers, which typically consist of interconnected neurons, are where the magic — or the transformation of data — happens. In its simplest form, within the classic *Multilayer Perceptron* (MLP) model, each hidden layer neuron performs a weighted operation:

$$\text{output} = f(w \cdot \text{input} + b)$$

- $\text{input} \in \mathbb{R}^d$ refers to the outputs from the previous layer (or the initial data from input nodes) that are fed into a specific neuron in the hidden layer.
- $w \in \mathbb{R}^d$ (weights) is a vector of parameters associated with that specific neuron, defining the importance of each input received by this neuron.
- $b \in \mathbb{R}$ (bias) is an additional scalar parameter specific to the neuron, which shifts the result of the weighted sum, allowing for more flexibility.
- $f(\cdot) : \mathbb{R} \rightarrow \mathbb{R}$ is the *activation function*, a nonlinear function applied to the weighted sum of inputs and bias in that specific neuron, allowing for more complexity.
- $\text{output} \in \mathbb{R}$ is the result produced by the neuron, which will then be passed on to the next hidden layer (or to the final output layer).

2 Background

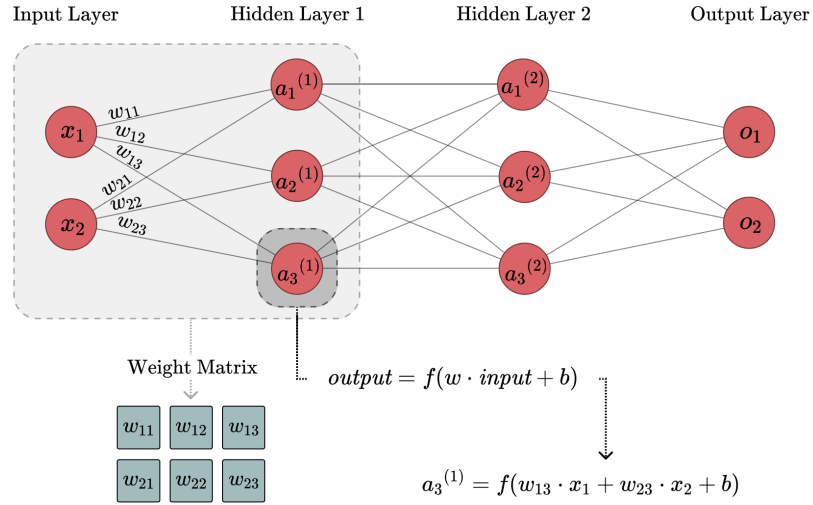


Figure 2.1: An example of an NN with two hidden dense layers, showing the connections between neurons in adjacent layers.

Hidden layers where each neuron is connected to every neuron in the previous layer and every neuron in the next layer are called *dense layers*. The *weight matrix* (W), which combines the weight vectors of all neurons in a dense layer, grows linearly with each added neuron or input node, embodying the interconnectedness of such layers

This interconnected structure introduces the inherent redundancy, or — in other words — the over-parameterization of NNs [12]. It is particularly true in models with a large number of neurons, where W results in a vast number of parameters, which do not contribute to the model accuracy equally [19].

Convolutional layers are another type of hidden layers that involve a *convolution* operation on the input. Intuitively, a standard convolution is a process of sliding a small grid, or *kernel*, over an input to find patterns. Figure 2.2, for example, shows the application of the Sobel kernel that detects edges on the input image. For multi-channeled inputs, like RGB images, the convolution operation uses a multi-channeled kernel, as shown in Figure 2.3, producing a single-channeled feature map that combines weighted contributions from all input channels. A convolutional layer includes multiple such kernels, generating feature maps equal to the number of kernels. After the convolution operation generates the feature maps, a bias term is added to each map, and the activation function is applied element-wise. Mathematically, a convolutional layer can be represented as:

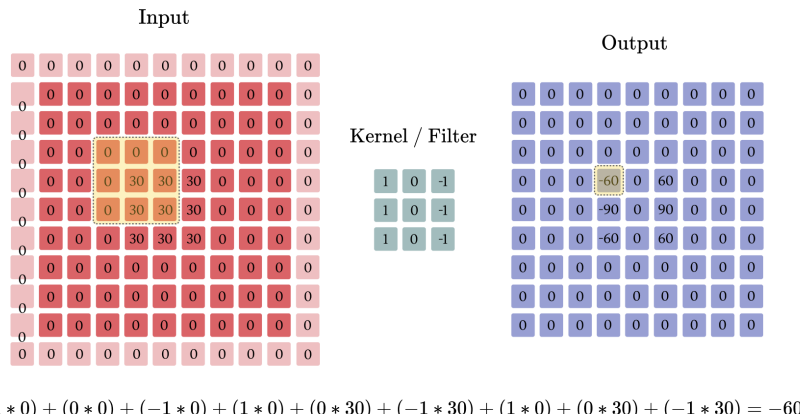
$$y_{i,j,k} = f \left(\sum_{m=1}^c \sum_{p=1}^h \sum_{q=1}^w x_{i+p-1,j+q-1,m} \cdot w_{p,q,m,k} + b_k \right)$$

- h, w are the height and width of the filter, respectively.
- c is the number of input channels.

2.1 Fundamentals of Deep Learning

- $y_{i,j,k}$ denotes the output at position (i, j) for the k -th filter.
- $x_{i+p-1,j+q-1,m}$ is the input at position $(i + p - 1, j + q - 1)$ for the m -th input channel.
- $w_{p,q,m,k}$ is the weight of the k -th filter at (p, q) for input channel m .
- b_k is the bias for the k -th filter.
- $f(\cdot) : \mathbb{R} \rightarrow \mathbb{R}$ is the activation function.

In other words, a convolutional layer applies filter weights as it slides over rows (p), columns (q), and channels (m), sums the results, adds bias (b_k), and repeats this for all positions (i, j) and filters (k) .



$$(1 * 0) + (0 * 0) + (-1 * 0) + (1 * 0) + (0 * 30) + (-1 * 30) + (1 * 0) + (0 * 30) + (-1 * 30) = -60$$

Figure 2.2: A 3×3 kernel sliding over a padded input matrix to compute the output feature map.

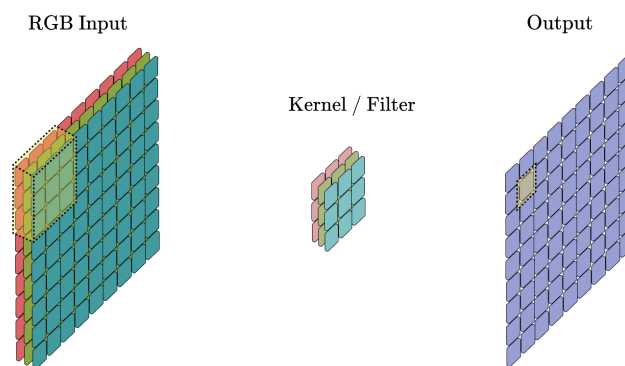


Figure 2.3: A $3 \times 3 \times 3$ kernel (filter) sliding over an RGB input matrix to produce a single-channeled output feature map.

2 Background

Although convolutional layers often have fewer weight parameters than dense layers in typical architectures, they still contain redundancies [17], presenting an opportunity for quantization. Together, dense and convolutional layers form the building blocks of convolutional neural networks (CNNs), the core of breakthroughs in computer vision [27, 28, 42]. Thus, both dense and convolutional layers will be the focus of this work.

2.1.2 Loss Functions and Regularization

The weights and biases of NN layers are usually *learnable parameters* that the model adjusts during *training*. The training process of NNs is similar to how our brains learn from mistakes. Given the ground truth, an NN adjusts its learnable parameters using a specific function that compares the ground truth with the output generated by the network, essentially measuring the magnitude of the network’s errors.

This function is called a *loss function*, and depending on the type of question the network aims to answer, it can take many different forms. For example, for the MLP described in Figure 2.1 that generates a binary classification, we would use the *log loss* function. Since the datasets used in this thesis involve multi-class classification, the *sparse categorical cross-entropy* (SCCE) loss function will be used, which measures the difference between the predicted class probabilities and the true labels for each class.

The loss function alone cannot ensure a neural network generalizes well to unseen data, as it focuses solely on minimizing error on the training set, which can lead to overfitting or a failure to capture the desired generalization properties. To mitigate overfitting, a *regularization term* is added to the loss function to penalize unwanted behaviors.

A typical regularization term is L_2 , which penalizes large weights by adding the sum of the squared weights to the loss. The modified loss function is then expressed as:

$$\mathcal{L}_{\text{total}} = \mathcal{L}_{\text{task}} + \lambda \sum_i w_i^2$$

- $\mathcal{L}_{\text{task}}$ is the original task-specific loss function (in our case, the SCCE loss function).
- λ is a scalar parameter that controls the strength of the regularization.
- w_i represents each individual weight value in the model.

Regularization terms may have different objectives, be it for better generalization, improved robustness, or encouraging sparsity in the model parameters. The current work employs multiple custom regularization terms that encourage quantization that we will discuss in detail in Section 3.2.

2.1.3 Forward-Pass and Back-Propagation

The repetition of the mathematical operations described earlier in Subsection 2.1.1 during model training constitutes the *forward pass*, the process where input data is passed through the network layer by layer, with each layer applying its learned weights and biases to produce a final output. This output is then compared with the ground truth by the loss

function that produces an error as explained in Subsection 2.1.2. The error is then used to update the parameters in W and b during a process called *back-propagation*. In other words, back-propagation is the method by which the network adjusts its parameters to minimize the error. This method calculates the gradient of the loss function with respect to each parameter using the chain rule. W and b are updated as follows:

$$W = W - \eta \frac{\partial L}{\partial W}, \quad b = b - \eta \frac{\partial L}{\partial b}$$

where L is the loss function, and η is the learning rate.

For example, consider the weight $w_{1,1}$ represented as the line between x_1 and the hidden layer node $a_1^{(1)}$ in Figure 2.1. The gradient of this weight with respect to the loss is calculated using the chain rule, as shown below:

$$\frac{\partial L}{\partial w_{1,1}} = \frac{\partial L}{\partial o_1} \cdot \frac{\partial o_1}{\partial a_1^{(1)}} \cdot \frac{\partial a_1^{(1)}}{\partial w_{1,1}}$$

- $\frac{\partial L}{\partial o_1}$ is the gradient of the loss with respect to o_1 .
- $\frac{\partial o_1}{\partial a_1^{(1)}}$ is the gradient of o_1 with respect to the output of $a_1^{(1)}$.
- $\frac{\partial a_1^{(1)}}{\partial w_{1,1}}$ is the value of x_1 , since $a_1^{(1)}$ is a weighted sum of the inputs.

The chain rule, and consequently backpropagation, is a critical bottleneck for quantization. This issue, along with its solution, will be detailed in Section 2.3.

2.2 Basics of Quantization

This section aims to motivate the use of quantization and further provides a broader understanding of the term regarding its types.

2.2.1 Purpose and Definition

As we become increasingly dependent on deep learning models disguised as everyday tools, the need for these models to function in a resource- and time-efficient manner is more imperative than ever. The focus on resource efficiency is particularly important, with the research community expressing concerns regarding the environmental effects of large models, the exponential size growth of which continues to significantly outpace that of system hardware [44]. In this regard, studies have examined quantization within the context of Green AI as a method to reduce the carbon footprint of ML models [40].

Aside from the environmental considerations, the mere need to reduce the computational cost and speed of predictive models comes as an apparent business requirement. This requirement is essential when — quite ironically — embedded systems, famous for their compactness, meet ML models, recognized for their complexity. Microcontrollers,

2 Background

for instance, usually are not able to perform floating-point operations, which must therefore be emulated in software, introducing significant overhead. For this reason, quantization, the process which reduces the memory footprint of a model, is also extensively covered in the realm of embedded systems that inherently prefer integer arithmetic, as well as bitwise operations [1, 35, 39, 47].

Another motivation for quantization — although somewhat controversial — is the fact that reducing the bit width of ML models makes them robust to adversarial attacks in certain cases [30]. This holds significant value in fields, such as autonomous driving, where model vulnerability may result in fatal outcomes. Interestingly enough, the use cases where such robustness is required also demand fast inference, as they rely on real-time predictions. Consider healthcare diagnostics needed for emergency scenarios or military defense mechanisms designed for immediate action.

The reasons for employing quantization are numerous and varied, but regardless of the motivation, the essence of the term itself — rooted in the early 20th century — remains unchanged: quantization refers to the division of a quantity into a discrete number of small parts [13]. With regard to ML models, quantization describes the process of dividing higher bit-width numbers into a discrete number of lower bit-width representations without causing significant degradation in accuracy [12].

Since ML models are generally considered redundant or over-parameterized, there are multiple points where quantization can be applied. Specifically, we apply quantization to the weights and biases of dense layers, as well as the kernels and biases of convolutional layers. Other applications include, but are not limited to, layer activation and layer input quantization (two sides of the same coin), as well as gradient quantization. The bottom line is that wherever there is an opportunity for arithmetic or memory optimization, there is room for quantization.

2.2.2 Core Quantization Approaches

There is a multitude of ways to classify NN quantization methods, a broader overview of which will be covered in Chapter 5. For now, we will focus on a few basic approaches from the general categories of both *data-driven* and *data-free* methods [46] to provide a basic understanding of the NN quantization process.

A basic form of data-free quantization, or *post-training quantization* [22], involves converting already trained parameters from FP32 to a lower bit-width format without using the initial training data. One approach is to apply *uniform quantization* that maps real values to a set number of *bins*. The formula can be written as:

$$Q(r) = \left\lfloor \frac{r}{S} \right\rfloor$$

- $Q(\cdot)$ denotes the quantization operation.
- r is the real value of a given model parameter in higher bit-width representation.
- S is a scaling factor.

As a result, we end up with values that can directly be cast to a lower bit-width representation, forming a discrete set of bins instead of an almost continuous range of real numbers, as shown in Figure 2.4.

Unlike data-free quantization — as the name suggests — data-driven quantization involves retraining the model using the initial data. An example of this approach is the Ristretto framework [14], which, similar to data-free methods, first analyzes the trained model to select suitable lower bit-width number formats for its weights. Then, using a portion of the original dataset, the framework determines appropriate formats for layer inputs and outputs. As a next step, based on the validation data, Ristretto adjusts the quantization settings to achieve optimal performance under the given constraints. Finally, the quantized model is fine-tuned using the training data.

A basic example of data-driven quantization is min-max quantization on input data, as shown in Figure 2.5, using the formula for 8-bit quantization:

$$Q_{\text{MinMax}}(x) = \left\lfloor \frac{x - \min(X)}{s} \right\rfloor, \quad \text{where } s = \frac{\max(X) - \min(X)}{2^8 - 1}$$

This method can also be implemented in a data-free scenario to quantize learned model parameters and is internally used as one of the default techniques in popular ML frameworks like Tensorflow and PyTorch.

Previously, we discussed *where* quantization could be applied in a model, mentioning weights, kernels, and biases as the focus of this thesis. Figure 2.4 and Figure 2.5 show examples of quantization using a scalar scaling factor. However, scaling factors can be applied at varying levels of detail, bringing forth the concept of *quantization granularity*.

Granularity refers to the level of detail at which *quantizers* — such as scaling factors, offset adjustments, or other binning strategies — are applied, ranging from a single quantizer for an entire kernel (coarse granularity) to separate ones for individual spatial locations, channels, or filters (fine granularity).

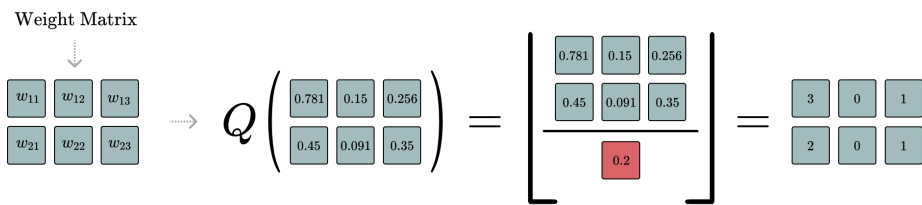


Figure 2.4: Uniform quantization of an arbitrary weight matrix.

2 Background

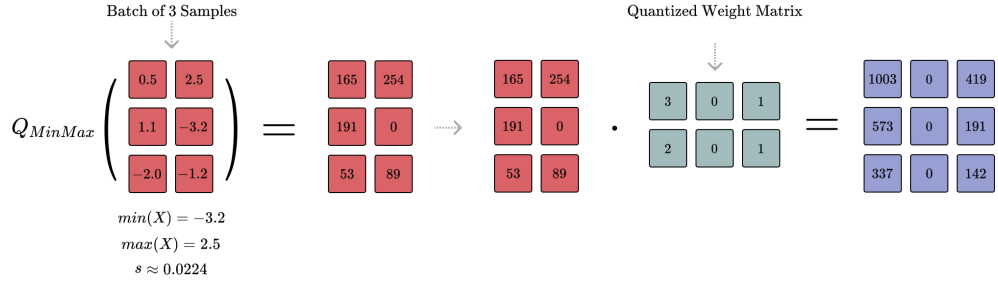


Figure 2.5: Min-max quantization of input data to 8 bits, followed by matrix multiplication with the quantized weight matrix.

Figure 2.6 illustrates various scaling factor granularities for the kernels of convolutional layers. Despite this wide range of possibilities, channel-wise quantization is currently the standard for convolutional layers [12], as it helps parallel processing capabilities of accelerators that compute channel outputs independently. For dense layers, row-wise quantization (one scaling factor for weights used by a single output neuron) is more prevalent because it aligns with matrix-vector multiplication, which then can be carried out by specialized linear algebra libraries in an optimized way [24]. Thus, in the experiments, we focus our quantization methods on channel-wise granularity for convolutional layers and row-wise granularity for dense layers, while also exploring a few additional applications.

2.3 Learned Quantization

Now that the fundamentals of quantization have been covered, this section introduces key concepts commonly encountered in learned quantization, including its challenges, trade-offs, and the popular techniques used to overcome them.

2.3.1 Trade-offs and Challenges

The inherent — or rather the widely accepted — characteristic of quantization is that it negatively influences accuracy. The trade-off between quantization and generalization refers to the balance of how much accuracy we are willing to sacrifice to gain a reduction in computational cost, memory usage, or inference time. However, the truth is that we usually cannot afford sacrificing anything. This challenge, coupled with the lack of a guarantee that predefined quantizers can yield optimal results [11, 47], has paved the way for the burgeoning field of learned quantization, which aims to *learn* how to quantize the model in a manner that mitigates performance loss.

Learned quantization is, however, a double-edged sword in the sense that, despite producing compact results, the cost to achieve them is higher [37]. The obvious reason

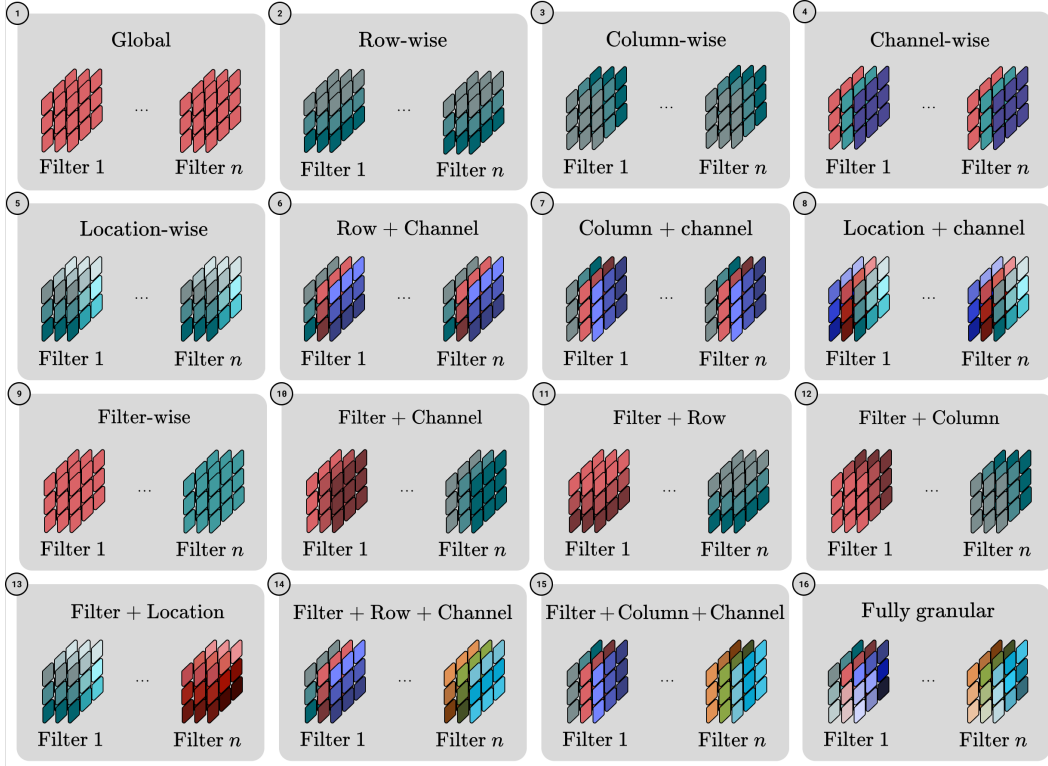


Figure 2.6: Various applications of scaling factors, ranging from a single scalar applied to the entire kernel (1) to separate scalars assigned to spatial dimensions (e.g., 1, 2), channels (4), filters (9), and other granular configurations.

is the additional computational overhead introduced by learnable quantizers. Thus, it is important to strike a balance between learning optimal quantization and keeping the training process manageable — which explains the prevailing emphasis on simplicity in most learned quantization research.

The main issue in achieving this simplicity is posed by the fact that discretization, in its essence, is non-differentiable — meaning it is challenging to integrate any kind of discretizing operations into gradient-based optimization methods, upon which ML models rely. Using the chain rule back-propagation example from Subsection 2.1.3, let us consider a simple flooring operation introduced into the process to better understand the problem. Suppose we quantize activations and apply $\lfloor \cdot \rfloor$ to hidden layer outputs:

$$a_{1,q}^{(1)} = \lfloor a_1^{(1)} \rfloor$$

As a result, the chain rule becomes:

$$\frac{\partial L}{\partial w_{1,1}} = \frac{\partial L}{\partial a_{1,q}^{(1)}} \cdot \frac{\partial a_{1,q}^{(1)}}{\partial a_1^{(1)}} \cdot \frac{\partial a_1^{(1)}}{\partial w_{1,1}}$$

2 Background

where $\frac{\partial a_{1,q}^{(1)}}{\partial a_1^{(1)}}$ presents a challenge. Since $a_{1,q}^{(1)} = \lfloor a_1^{(1)} \rfloor$, the derivative is:

$$\frac{\partial a_{1,q}^{(1)}}{\partial a_1^{(1)}} = \begin{cases} 0 & \text{if } a_1^{(1)} \notin \mathbb{Z}, \\ \text{undefined} & \text{if } a_1^{(1)} \in \mathbb{Z}. \end{cases}$$

This means that for most values of $a_1^{(1)}$, which are non-integer, the gradient becomes 0, resulting in $w_{1,1}$ not receiving any updates. For integer values of $a_1^{(1)}$, the back-propagation process fails altogether.

In essence, circumventing the issue of non-differentiability is the fundamental problem that learned quantization aims to solve, all while managing the aforementioned trade-offs to produce a model that is compact, not overly complex to train, and highly performant.

2.3.2 Common Methods

The most common method to address the issue of non-differentiability is to approximate the gradient of quantization operators using the Straight-Through Estimator (STE) [2, 41, 47]. This workaround applies the quantization operation *as is* during the forward-pass, but replaces the gradient of the piece-wise discontinuous function with that of a continuous identity function. Returning to the example from the previous subsection, if we apply the STE to the problematic gradient, instead of:

$$\frac{\partial a_{1,q}^{(1)}}{\partial a_1^{(1)}} = \begin{cases} 0 & \text{if } a_1^{(1)} \notin \mathbb{Z}, \\ \text{undefined} & \text{if } a_1^{(1)} \in \mathbb{Z}. \end{cases}$$

we approximate it as:

$$\frac{\partial a_{1,q}^{(1)}}{\partial a_1^{(1)}} \approx 1$$

This approximation enables gradient flow, allowing model parameters to receive updates without being hindered by the non-differentiability of the quantization step.

The STE — and other estimators [4] — are the cornerstone of quantization-aware training (QAT) [21], a subfield that falls under the broader umbrella of learned quantization. QAT, however, does not necessarily focus on learning quantization parameters. Instead, it focuses on helping the model adapt to the loss caused by the quantization process during the forward pass, whether or not trainable quantizers are involved.

More often than not QAT and trainable quantization parameters are combined. An example is quantization-interval-learning (QIL) [23], which uses three trainable quantization parameters (the center of the interval, the distance to the center, and a parameter that controls the scaling itself) with piecewise differentiable operations and relies on STE for gradient updates of quantized weights and activations. Similarly, the learned step size quantization (LSQ) approach [11] defines a single trainable quantization parameter (step size) with an explicit gradient formula and also uses STE for standard parameter updates. LQ-Nets [47] depend on STE too, but — unlike the two previous techniques — directly

2.3 Learned Quantization

incorporate a quantization error minimization algorithm to calculate binary encodings and the associated bases of model parameters given a predefined bit size.

Another way to achieve learned quantization is through the use of a regularization term. Such regularization terms are often periodic functions, such as sinusoidal functions [8, 34], which pull model parameters toward the nearest step — or quantization bin. A notable example is WaveQ [9], which combines a sine regularizer with an additional term that encourages lower bit widths without predefined bit constraints. A more straightforward regularizer is the Mean Squared Quantization Error [6] that directly minimizes the difference between the high-precision parameters and their quantized counterparts.

In this thesis, we will utilize STE but introduce a custom gradient calculation for the scale factor gradients based on a specific type of gradient sensitivity in the model parameters. Additionally, we will explore custom loss regularization terms that encourage quantization and systematically compare them across different datasets.

2 Background

3 Learned Quantization Schemes

This chapter introduces two custom learned quantization schemes — approaches that allow models to learn to quantize with adjustable intensity. The first one, a custom quantization layer featuring a threshold for gradient-based scale updates, will be discussed in Section 3.1. The second scheme, which focuses on custom regularization terms with a configurable penalty rate, will be covered second in Section 3.2.

3.1 Nested Quantization Layer

To separate the quantization logic from the usual structure of NN layers, we define a nested quantization layer that can be used within a standard one. This approach provides usability, making it easy to extend the functionality to other types of layers beyond dense and convolutional ones. We will first explain the core logic of the nested quantization layer and how it integrates into a model, followed by a detailed explanation of how the trainable scaling factors are updated.

3.1.1 Core Logic and Structure

As the name "nested quantization layer" suggests — this layer is implemented in a way that it is initialized from within a model layer itself. To explain, let P be the parameters of a layer (weights, bias or kernel). This P is used as the input for the nested quantization layer, where it undergoes quantization based on a scaling factor s . In turn, s is the only trainable parameter of the nested layer itself. The forward-pass of the nested layer performs the following operation:

$$P_{\text{reconstructed}} = P_{\text{quantized}} \cdot s$$

where $P_{\text{quantized}}$ is the quantized integer form of P and is defined as:

$$P_{\text{quantized}} = \left\lfloor \frac{P}{s} \right\rfloor$$

During back-propagation, the nested layer receives the upstream gradient of $P_{\text{reconstructed}}$ and passes it downward as is. This follows the standard STE behaviour used with non-differentiable discretizers, such as $\lfloor \cdot \rfloor$ in our case, as discussed in Subsection 2.2.2.

For updating the scale factor s — its own trainable parameter — the nested layer utilizes the upstream gradient of $P_{\text{reconstructed}}$ and applies a custom logic, which will be detailed in Subsection 3.1.2. Essentially, this approach solves two problems with one tool — updating both P and s using the same gradient, though with different logic.

3 Learned Quantization Schemes

Conceptually, the resulting structure with one or more nested quantization layers is illustrated in Figure 3.1 on the example of a convolutional layer.

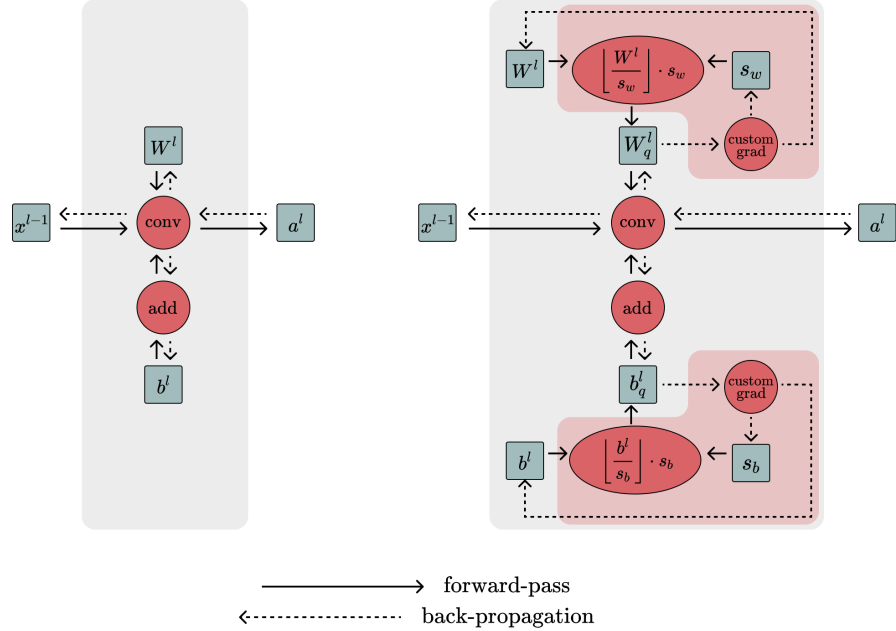


Figure 3.1: A convolutional layer (left) and its integration with the nested quantization layer (right) for both weights and bias. Trainable scaling factors are updated using custom gradients. Parameter gradients are passed downward as is.

Since the scaling factor s can have different shapes and be applied at varying levels of granularity, we have enabled scalar, row-wise, and column-wise application granularity for dense layers, as shown in Figure 3.2. For convolutional layers, we additionally support channel-wise granularity, corresponding to the first four scenarios in Figure 2.6.

The nested layer is built upon Tensorflow's `tf.keras.Layer` class, which serves as the base for all Keras layers. The gradient calculation logic is wrapped in Tensorflow's `tf.custom_gradient` decorator, allowing proper functioning of the model's computational graph. Dense and convolutional layers have been implemented as `tf.keras.Layer` objects with minimal adjustments as well to incorporate the nested layers logic.

3.1.2 Learned Scale Factor

For the trainable scale factor s , we define a custom gradient formula. The gradient of the loss with respect to s , denoted as $\nabla_s L$, is computed as:

$$\nabla_s L = g_s \cdot m$$

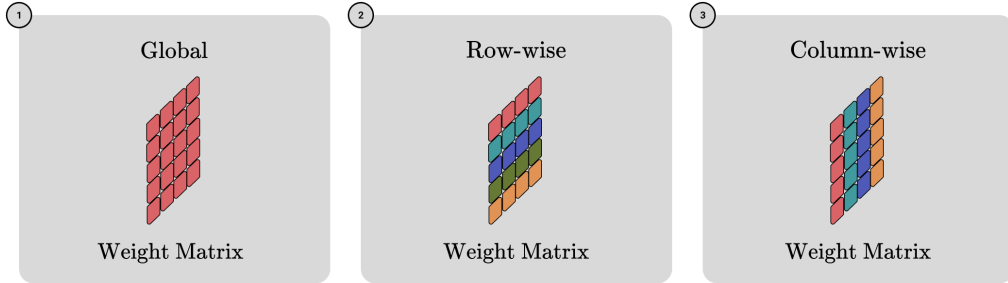


Figure 3.2: Various applications of scaling factors, ranging from a single scalar applied to the entire weight matrix (1) to row-wise and column-wise application of vector scalers.

Let us consider both multiplication terms separately. g_s is the main "decision maker" on whether to increase the scale and, therefore, quantize more. g_s is calculated using a hyperparameter threshold λ , which is compared against the ratio r .

$$g_s = \begin{cases} 0, & \text{if } r \geq \lambda \\ -\tanh(\lambda - r), & \text{if } r < \lambda \end{cases}$$

In turn, r is the ratio between the upstream gradient of the layer's reconstructed parameter $P_{\text{reconstructed}}$ with respect to the loss and its absolute value (for simplicity, we denote $P_{\text{reconstructed}}$ as P_r):

$$r = \frac{|\nabla_{P_r} L|}{\max(\epsilon, |P_r|)}$$

The formula conveys the relative impact of the gradient on the parameter's value. A large r indicates that the parameter is not ready for intense quantization because small perturbations can lead to significant changes in its optimization. Conversely, parameters with a small r are better candidates for quantization since they are less sensitive.

The decision to replace P_r with ϵ when $P_r = 0$ ensures that the corresponding r becomes large, effectively resisting quantization. This behavior is valid regardless of the parameter's sensitivity — if the zero parameter is sensitive, quantization could disrupt future optimization steps, and if it is not sensitive, quantization adds no value since s has a positive non-zero constraint and $\frac{P}{s}$ will remain zero.

The motivation behind using $\tanh(\cdot)$ primarily stems from two key reasons. First, $\tanh(\cdot)$ is bounded (in our use case, to $[-1, 0]$), which prevents excessive gradient magnitudes. Second, unlike sigmoid, the hyperbolic tangent does not require any additional rescaling since it is symmetric around 0. An additional point is that $\tanh(\cdot)$ saturates comparably faster than the sigmoid function, potentially allowing for more decisive gradients, but it is uncertain how much influence this has.

Now that g_s is covered, let's take a look at m defined as:

$$m = \max(|P_{\text{quantized}}|)$$

3 Learned Quantization Schemes

where the shape of m corresponds to the shape of s . For example, if s is a row-wise scalar, then m will hold the maximum value from each row of $|P_{quantized}|$. Similarly if s is a single scalar value, then m represents the maximum across the entire layer parameter.

A larger m indicates a wider range of quantized values, implying the parameter can tolerate coarser quantization. In contrast, a smaller m means a narrower range, where intense quantization could be rather harmful. As a result, by multiplying g_s with m , the adjustment to the scale becomes proportional to the parameter's range. This encourages coarser quantization for parameters with larger ranges while being conservative for smaller ones.

To sum this part up, the intuition is that the gradient adjustment for the scale factor s adapts dynamically based on both the sensitivity of the parameter g_s and its range m . Sensitive parameters are left with a "zero vote", while the less sensitive ones have a say on how much quantization they can tolerate.

In cases where all parameters are deemed sensitive with $r \geq \lambda$ and $g_s = 0$, the scale factor s does not receive gradient updates. Such a situation could result in an unfavorable outcome where the parameters themselves increase in magnitude while the scale factor remains unchanged, loosening the achieved quantization. To address this, we apply a small constant update tied to λ in cases where all parameters have $r \geq \lambda$. As a result, the initial formula for g_s becomes:

$$g_s = \begin{cases} -\tanh(\lambda), & \text{if } \forall P_r, r \geq \lambda \\ -\tanh(\lambda - r) \cdot \mathbf{1}(r < \lambda), & \text{otherwise} \end{cases}$$

Finally, the scale gradients are initially calculated for each parameter value but are then aggregated along the corresponding granularity axes. This aggregation reflects the collective behavior of parameters within the same granularity, where only those deemed quantizable and with a meaningful "say" contribute to the overall adjustment, while sensitive parameters express their resistance with a "zero vote". Even when all parameters are sensitive and each casts a "zero vote", we still force the "elections" by introducing a constant gradient term to avoid stagnation in scale factor updates.

In Chapter 4, we will present experimental results for different values of λ , offering guidance on the optimal values for both dense and convolutional layers.

3.2 Custom Loss Function Terms

Building on the nested quantization layers covered in Section 3.1, we define three custom loss function terms that can be used in combination with the task-specific loss. We will first explain how these terms fit into the model's structure and training process, then provide the details of their individual formulations.

3.2.1 Design and Integration

To incorporate custom loss terms into the model's training process, we utilize the nested layers described in Section 3.1, with a slight modification. The modification lies in the

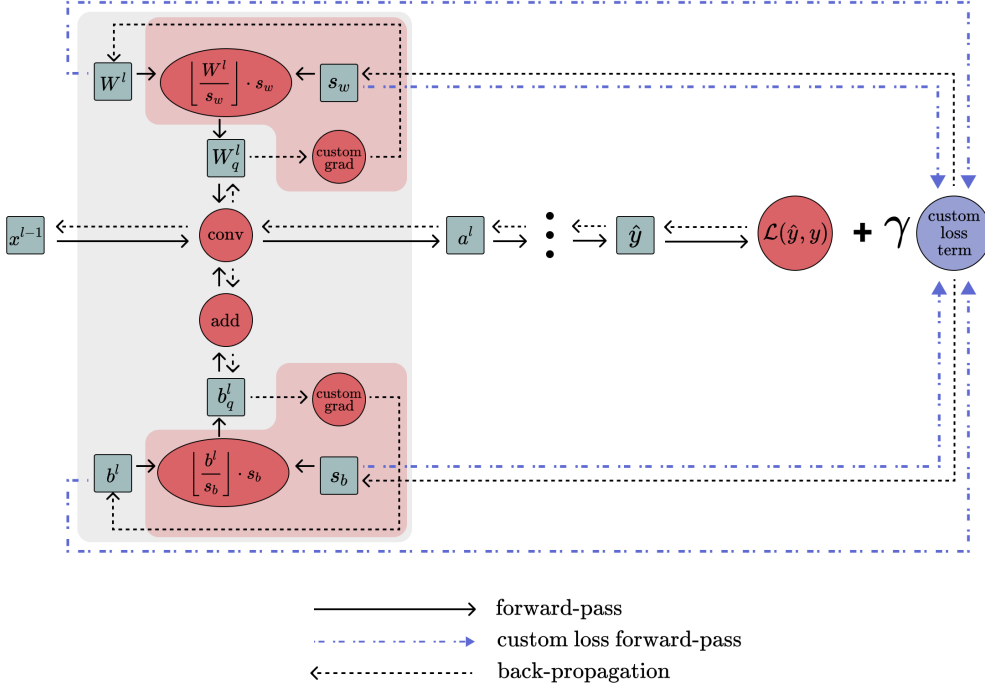


Figure 3.3: Custom loss term using scale factors and model parameters integrated into training.

gradient calculation of the nested layers, where we similarly use STE for parameter updates, but do not provide any gradient updates for the scale factors altogether. This is equivalent to setting $\lambda = 0$, which disables gradient updates for the scale factors.

Instead, to update scale factors, we define a custom loss term $\mathcal{L}_{\text{custom}}$ scaled by a penalty rate γ , an adjustable hyperparameter. This loss term depends on the model parameters and scale factors and is added to the task-specific loss:

$$\mathcal{L}_{\text{total}} = \mathcal{L}_{\text{task}} + \gamma \cdot \mathcal{L}_{\text{custom}}$$

As visualized in Figure 3.3, scale factors receive gradient updates from the custom loss term, while the gradients for model parameters are influenced by both the task-specific loss and the custom loss term. To illustrate this process further, if we set $\gamma = 0$, the scale factors will not receive any updates, and the model will rely on the STE to adapt to the initial values of the scale factors during training.

The custom loss terms are implemented as Python objects to which the model's nested quantization layers are passed. These objects have access to the latest values of parameters and scale factors at any point during training.

Unlike the method described in Section 3.1, this approach defines a forward-pass to calculate the custom loss terms, rather than manipulating gradients directly. As a result, it may appear more straightforward and will be shown to achieve equally good results..

3 Learned Quantization Schemes

3.2.2 Loss Term Definitions

We use the same notation, with P representing the parameters of a nested quantization layer (weights, bias or kernel) and s as the corresponding scale factor. Additionally, we denote the elements in the scale factor s as $\{s_1, \dots, s_K\}$.

MaxBin Penalty. We name the first custom loss term MaxBin Penalty and define the function $\text{maxbin}(P, s)$ as the collection of per- s_k maxima:

$$\text{maxbin}(P, s) = \left(\max_{(i,j):s_{i,j}=s_k} \frac{|P_{i,j}|}{s_k} \right)$$

where $P_{i,j}$ is an element of P , and $s_{i,j}$ — the corresponding scaling element. The result is of the same shape as s and conveys the maximum bin value, or range, for each s_k . For the weights W^l and bias b^l of a nested quantization layer indexed by l , we apply $\text{maxbin}(\cdot)$ to compute the maximum bin values relative to s_W^l and s_b^l :

$$\text{bin_max}_{W^l} = \text{maxbin}(W^l, s_W^l), \quad \text{bin_max}_{b^l} = \text{maxbin}(b^l, s_b^l)$$

We then calculate the layer-specific MaxBin penalty $\mathcal{L}_{\text{MaxBin}}^l$ as the weighted sum of the mean maximum bin values for W^l and b^l , scaled by their total number of parameters:

$$\mathcal{L}_{\text{MaxBin}}^l = \#(W^l) \cdot \text{mean}(\text{bin_max}_{W^l}) + \#(b^l) \cdot \text{mean}(\text{bin_max}_{b^l})$$

where $\#(W^l)$ and $\#(b^l)$ represent the total number of parameters in W^l and b^l . As the next step, we sum these layer-wise penalties over all nested quantization layers $l \in L$, then normalize by the total number of parameters in those layers.

$$\mathcal{L}_{\text{MaxBin}} = \frac{\sum_{l \in L} \mathcal{L}_{\text{MaxBin}}^l}{\sum_{l \in L} (\#(W^l) + \#(b^l))}$$

In the end, we scale $\mathcal{L}_{\text{MaxBin}}$ with an adjustable penalty rate γ and integrate it into the loss objective as follows:

$$\mathcal{L}_{\text{total}} = \mathcal{L}_{\text{task}} + \gamma \cdot \mathcal{L}_{\text{MaxBin}}$$

where $\mathcal{L}_{\text{task}}$ represents the task-specific loss function, and γ controls the contribution of the MaxBin penalty to the total loss. Intuitively, the MaxBin penalty encourages larger scale factor values that result in a small quantization range, while discouraging the ones that result in higher bin values.

Inverse Penalty. We name the second custom loss term Inverse Penalty and define the function $\text{inverse}(s)$ as the mean of the inverse scale factor values:

$$\text{inverse}(s) = \text{mean}\left(\frac{1}{s_{i,j}}\right)$$

where $s_{i,j} > 0$, since s has a positive non-zero constraint. For the weights W^l and bias b^l of a nested quantization layer l , with scale factors s_W^l and s_b^l , the layer-specific inverse penalty is defined as:

$$\mathcal{L}_{\text{Inv}}^l = \#(W^l) \cdot \text{inverse}(s_W^l) + \#(b^l) \cdot \text{inverse}(s_b^l)$$

3.2 Custom Loss Function Terms

As the next step, we sum these penalties across all nested quantization layers $l \in L$, and normalize by the total number of parameters in those layers:

$$\mathcal{L}_{Inv} = \frac{\sum_{l \in L} \mathcal{L}_{Inv}^l}{\sum_{l \in L} (\#(W^l) + \#(b^l))}$$

Finally, we scale \mathcal{L}_{Inv} with an adjustable penalty rate γ and integrate it into the loss objective, just like we did with the MaxBin Penalty. Unlike the Maxbin Penalty, the Inverse Penalty directly encourages larger scale factors, without taking into account the resulting bin values.

Difference Penalty. We name the third custom loss term Difference Penalty and define the following function:

$$\text{difference}(P, s) = \text{mean}\left(\left|P - \frac{P}{s}\right|\right)$$

which measures the average absolute difference between the original parameters P and their scaled values, where s is the corresponding scale factor. For a nested quantization layer l with weights W^l and biases b^l , and their respective scale factors s_W^l and s_b^l , the layer-specific Difference Penalty is given by:

$$\mathcal{L}_{Diff}^l = \#(W^l) \cdot \text{difference}(W^l, s_W^l) + \#(b^l) \cdot \text{difference}(b^l, s_b^l)$$

Next, we sum these Difference Penalties across all nested quantization layers and normalize by the total number of parameters in these layers the same way we did for \mathcal{L}_{MaxBin} and \mathcal{L}_{Inv} . In the end we similarly add it to the task-specific loss scaled by γ . Intuitively, the Difference Penalty encourages larger scale factors, as smaller ones result in a greater difference between the original and scaled parameters, increasing the penalty.

To summarize, while these custom loss terms are the only source of gradient updates for the scale factors, weights and biases are updated both through the main task-specific loss and, where relevant, through the custom loss terms. The Inverse Penalty, for instance, affects only the scale factors and does not directly influence the weights or biases. We additionally note that during the forward-pass, parameters are quantized by their respective scale factors, with the STE ensuring that the weights and biases can adapt to the learned quantization in the backward-pass.

In Chapter 4, we will present the comparison of the three loss terms and provide guidance on the optimal values of γ .

3 Learned Quantization Schemes

4 Experiments

This chapter details the experiments conducted in the context of this thesis. We evaluate the proposed methods on three image classification datasets: MNIST [29], CIFAR-10 [26], and Imagenette [16], which is a subset of 10 easily classified classes from the ImageNet dataset. First, we provide an overview of the experimental setup. We then present the results of the gradient ratio thresholding method, as detailed in Section 3.1, followed by the results of the custom loss terms discussed in Section 3.2.

4.1 Experimental Setup

Software and Hardware Setup. As briefly mentioned in Section 3.1, our custom methods are implemented in TensorFlow. Specifically, we used TensorFlow version 2.11.0, running on Python 3.10.14. All experiments are conducted on a server equipped with two NVIDIA A40 GPUs, each with 48 GB of memory, running on CUDA 11.4 and driver version 470.256.02.

Experiment Networks. For simplicity and tractability, we define custom networks for each dataset. For MNIST, we use a small network consisting of two dense layers, each adjusted to incorporate nested quantization layers for both weights and biases. For CIFAR-10, we use a convolutional network with three blocks of convolutional layers, each adjusted to incorporate nested quantization layers for both kernels and biases. These are followed by two dense layers. The Imagenette model is a ResNet-inspired architecture, featuring an initial quantized convolutional block followed by four stages of residual blocks. Each residual block incorporates the adjusted convolutional layers with nested quantization for both kernels and biases. For the experimentation with custom loss terms, we use equivalent networks without the nested quantization layer logic.

Table 4.1: Network Settings for Different Datasets

Hyperparameter	MNIST	CIFAR-10	Imagenette
Learning Rate	0.0001	0.0001	0.0001 ¹
Batch Size	32	128	64
Epochs	20	100	100
Seed for Reproducibility	42	42	42

¹ For Imagenette, the learning rate decays by 0.5 at epoch 40 and by 0.2 at epoch 60.

4 Experiments

Baseline Hyperparameters and Initialization. Using the hyperparameters described in Table 4.1, each network optimizes its parameters using the Adam optimizer and the sparse categorical cross-entropy loss function. Weights and biases are initialized with random normal values, while scale factors are initialized with very small constant values for all cases. Scale factors are constrained to be positive and non-zero to avoid numerical issues during division. An example implementation for reproducing these networks is available at the following GitHub link: <https://github.com/anuunchin/learned-quantization>

4.2 Analysis of Nested Quantization Layers

For the nested quantization layer method, we examine how the approach behaves under different thresholds λ for both dense and convolutional layers. The first subsection presents results for fully connected layers trained on MNIST, while the second subsection focuses on convolutional layers trained on CIFAR-10 and Imagenette.

4.2.1 Fully Connected Layers

As mentioned earlier, we use a small network with two dense layers trained on the MNIST dataset. These two dense layers have weight matrices W_1 and W_2 , along with bias vectors b_1 and b_2 . We examine three scenarios: applying the scale factor row-wise, column-wise, and as a single scalar for the entire weight matrix. For all scenarios, a scalar value is used as the scale factor for each bias. Table 4.2 shows the configurations.

The experiments have demonstrated that the optimal quantization is observed for a penalty threshold of $\lambda = 1e - 10$ across all three scenarios. This conclusion is based on Pareto front plots in Figure 4.1, which illustrate the trade-off between accuracy loss and quantization. We see that, for all scenarios, the number of unique integer values after quantization, aggregated across all parameters of the two dense layers, reaches its lowest point at $\lambda = 1e - 10$ without significantly degrading the accuracy.

As an example, the actual integer values after quantization for the rowwise scenario is depicted in Figure 4.2 for all four parameters separately. While the total number of unique values is only 24, the range spans from -12 to 11 . Consequently, 5 bits are sufficient to represent the quantized values in the resulting layers, as $\lceil \log_2(24) \rceil = 5$, covering all 24 unique values within the range. The bit requirement can be further reduced using

Table 4.2: Scale factor granularity for dense layers

Parameter	Row-wise	Column-wise	Scalar
W_1 (784, 128)	s (784, 1)	s (1, 128)	s (1, 1)
b_1 (128, 1)	s (1, 1)	s (1, 1)	s (1, 1)
W_2 (128, 10)	s (128, 1)	s (1, 10)	s (1, 1)
b_2 (10, 1)	s (1, 1)	s (1, 1)	s (1, 1)

4.2 Analysis of Nested Quantization Layers

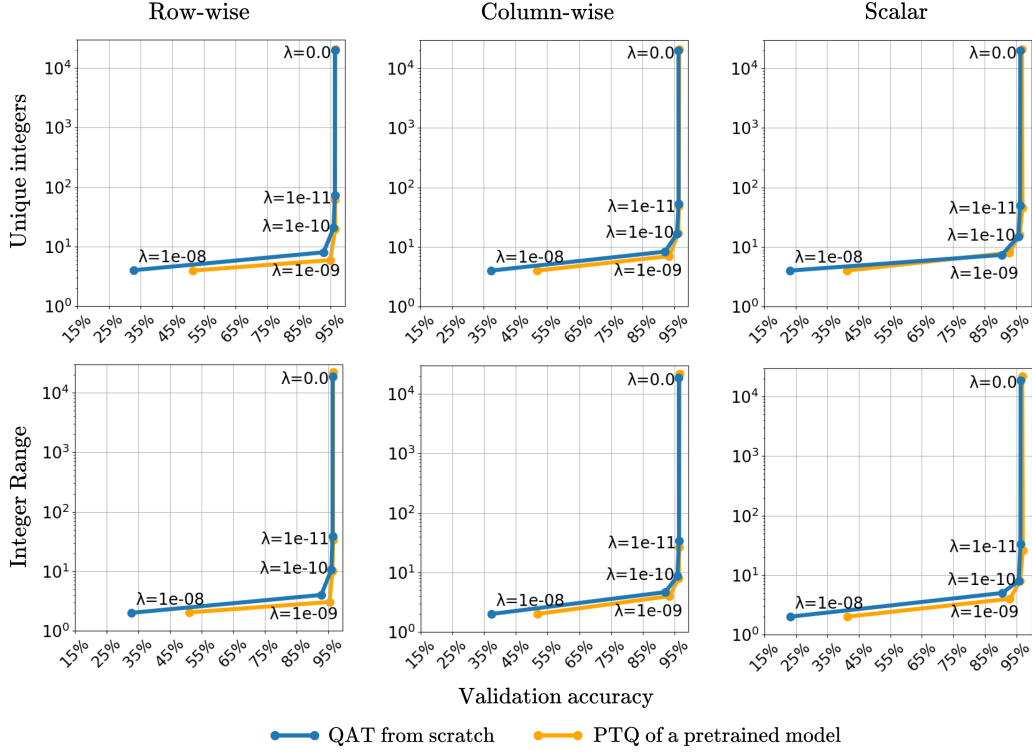


Figure 4.1: Accuracy – quantization trade-off for nested quantization layers on MNIST.

compression techniques like Huffman coding [20], considering the concentration of values around 0 in the distributions of quantized weights.

Interestingly, as depicted in Figure 4.3, the validation loss for $\lambda = 1e - 10$ consistently remains lower than the full-precision baseline and $\lambda = 0.0$ throughout the training process. At the same time, the validation accuracy remains almost identical to the baseline. This indicates that the penalty threshold of $\lambda = 1e - 10$ not only preserves the classification accuracy of the model but also improves generalization with regard to loss, making the model more confident in its predictions.

In terms of quantization granularity, we see that a scalar scaling factor applied to weights produces slightly worse results compared to row-wise and column-wise granularity. The steeper accuracy degradation and greater loss increase for $\lambda = 1e - 8$ demonstrate this effect, as shown in Figure 4.3. The suboptimal performance of the scalar scaling factor suggests that layer-wise quantization, which it represents, may be too coarse to account for the variability in parameter distributions within a layer. Therefore, finer granularities, such as row-wise or column-wise scaling, are more suitable candidates for optimal quantization granularity of dense layers.

We additionally consider a scenario where the full-precision baseline model is used to perform post-training quantization (PTQ) with the same set of values for λ . In this context, we note that the term PTQ should, in our specific scenario, be extended to

4 Experiments

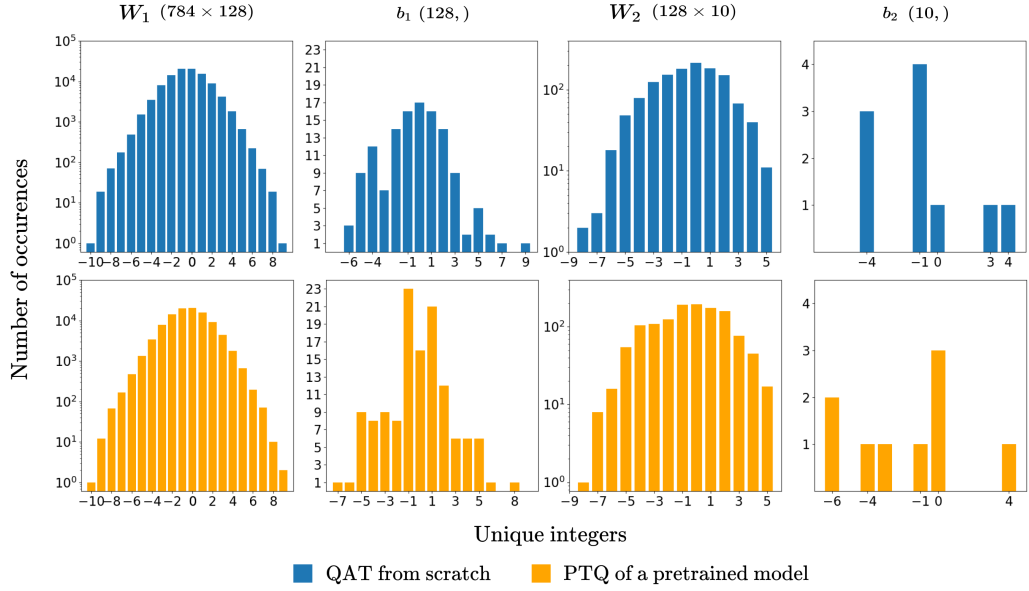


Figure 4.2: Quantization of MNIST dense layers with row-wise granularity at $\lambda = 1e-10$.

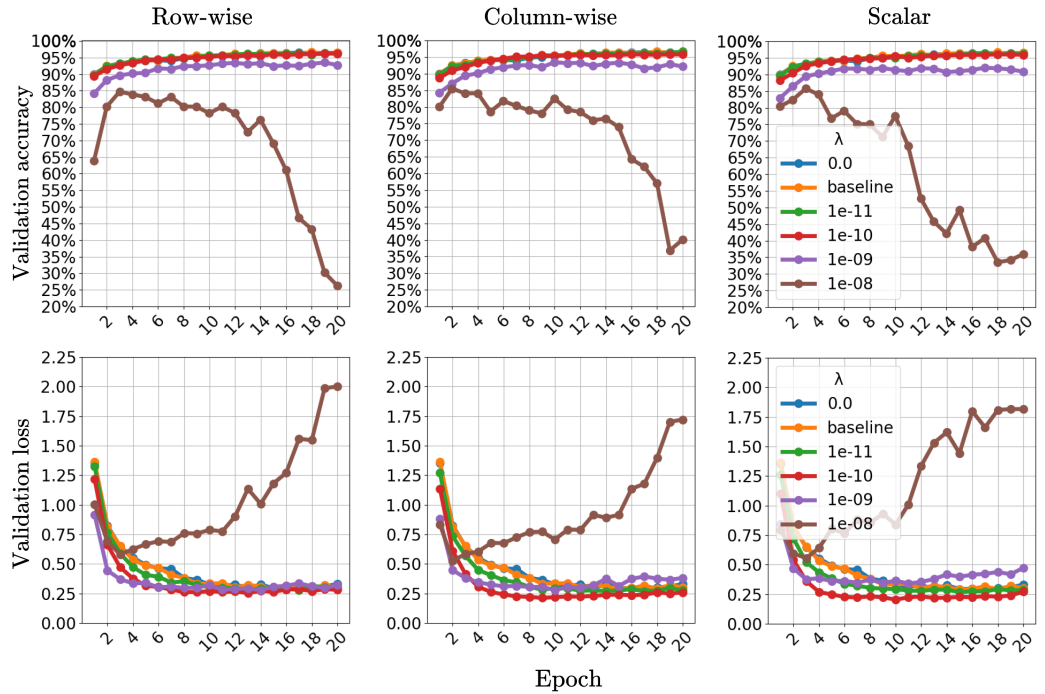


Figure 4.3: Impact of quantization on accuracy and loss for different λ on MNIST.

4.2 Analysis of Nested Quantization Layers

post-training quantization-aware training. However, for simplicity, we continue to use the term PTQ to clearly distinguish this approach from QAT performed from scratch.

As shown in Figure 4.1, we see that the Pareto fronts do not change significantly, with higher values of λ even achieving a slightly lower number of unique integers at the end compared to training from scratch. However, this small advantage is not major. As illustrated in Figure 4.4, this minor benefit occurs only when the model has already lost a significant amount of accuracy. Nevertheless, the previously defined optimal value of $\lambda = 1e - 10$ holds for PTQ as well, producing comparable results as shown in Figure 4.2

4.2.2 Convolutional Layers

For the CIFAR-10 dataset, we define a CNN, with six nested convolutional layers. Each convolutional layer has a kernel and a bias. We examine four scenarios: applying the scale factor channel-wise, row-wise, column-wise, and as a single scalar for the entire kernel. For all scenarios, a scalar factor is used for each bias vector, similar to how we quantized dense layers. The kernel configurations are shown in Table 4.3 for clarity.

The experiments show that the optimal value for the hyperparameter is $\lambda = 1e - 11$, across all four scenarios, as depicted in Figure 4.5. As an example, the integer values after quantization for the row-wise scenario across all quantized parameters range from -22 to 32 , resulting in 60 unique values that can be represented with $\lceil \log_2(60) \rceil = 6$ bits. The histograms of the resulting integer values in the kernels, displayed in Figure 4.6, form

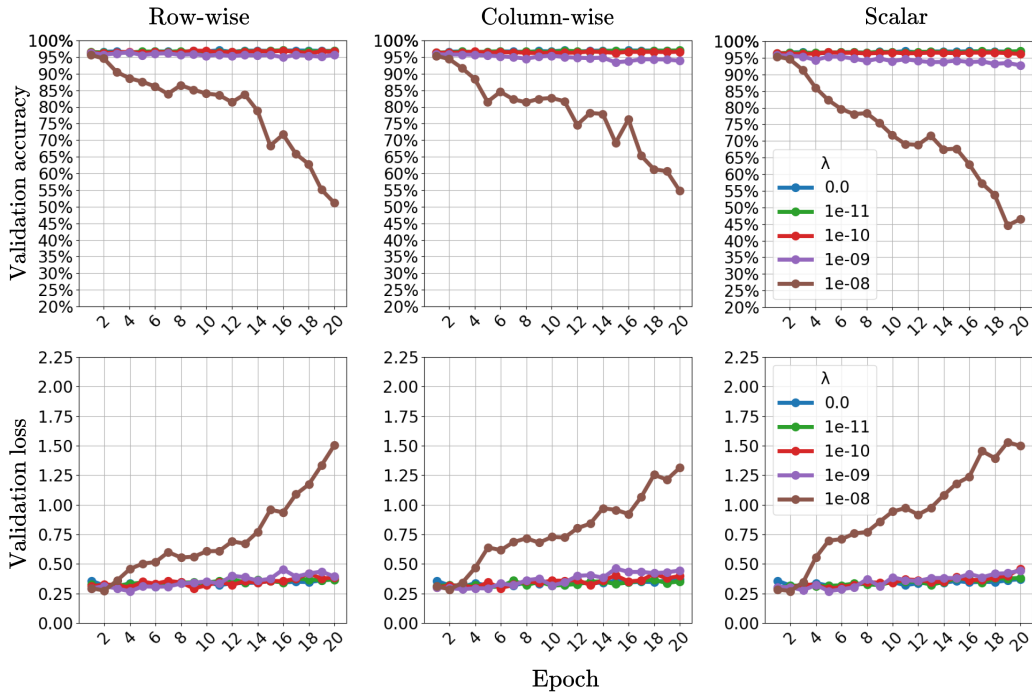


Figure 4.4: Impact of PTQ on accuracy and loss for different λ on MNIST.

4 Experiments

Table 4.3: Scale factor granularity for convolutional kernels

Kernel	Channel-wise	Row-wise	Column-wise	Scalar
$K_1 (3, 3, 3, 32)$	(1, 1, 3, 1)	(3, 1, 1, 1)	(1, 3, 1, 1)	(1, 1, 1, 1)
$K_2 (3, 3, 32, 32)$	(1, 1, 32, 1)	(3, 1, 1, 1)	(1, 3, 1, 1)	(1, 1, 1, 1)
$K_3 (3, 3, 32, 64)$	(1, 1, 32, 1)	(3, 1, 1, 1)	(1, 3, 1, 1)	(1, 1, 1, 1)
$K_4 (3, 3, 64, 64)$	(1, 1, 64, 1)	(3, 1, 1, 1)	(1, 3, 1, 1)	(1, 1, 1, 1)
$K_5 (3, 3, 64, 128)$	(1, 1, 64, 1)	(3, 1, 1, 1)	(1, 3, 1, 1)	(1, 1, 1, 1)
$K_6 (3, 3, 128, 128)$	(1, 1, 128, 1)	(3, 1, 1, 1)	(1, 3, 1, 1)	(1, 1, 1, 1)

Note: (1, 1, 1, 1) denotes a scalar, broadcasted across the kernel for consistency.

a bell curve similar to the experimental results for dense layer weights. If a slightly greater degradation in accuracy is viable, λ can be increased to $\lambda = 1e - 10$. In the row-wise case, this adjustment results in a reduced range of integers, spanning from -8 to 11 . Further increasing λ could reduce the number of unique values to less than ten.

From Figure 4.7, we do not observe a significant difference in performance between the row-wise, column-wise, channel-wise, and scalar granularity scenarios. This suggests that the gradient-based method for updating scale factors produces "votes" and aggregated updates that are largely consistent across granularities. As a result, the scale factors tend to converge to similar values. Therefore, the scalar granularity may be the most suitable choice, as it requires the fewest parameters and offers the simplest implementation.

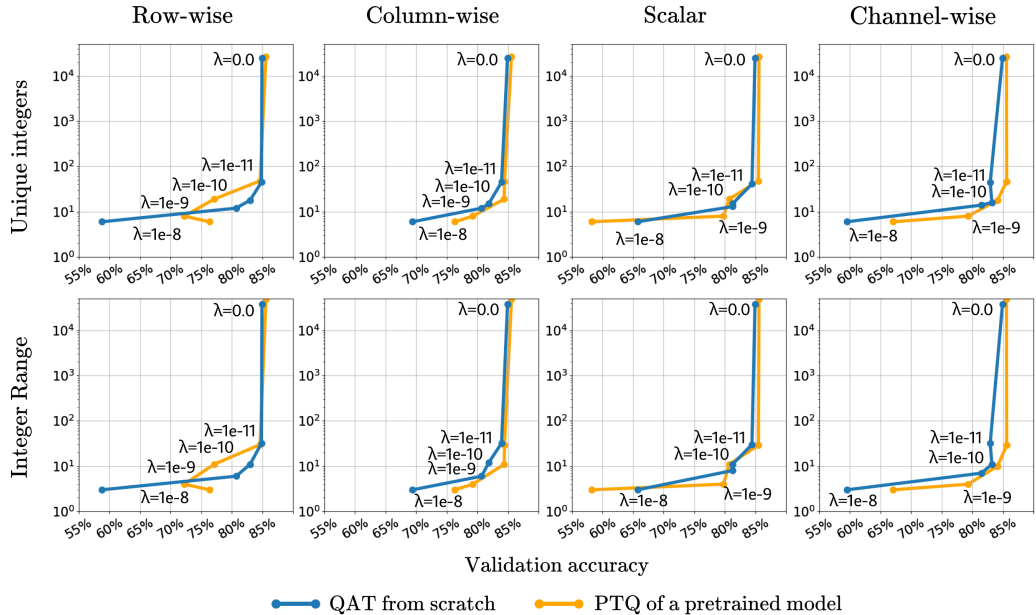


Figure 4.5: Accuracy-quantization trade-off for nested quantization layers on CIFAR-10.

4.2 Analysis of Nested Quantization Layers

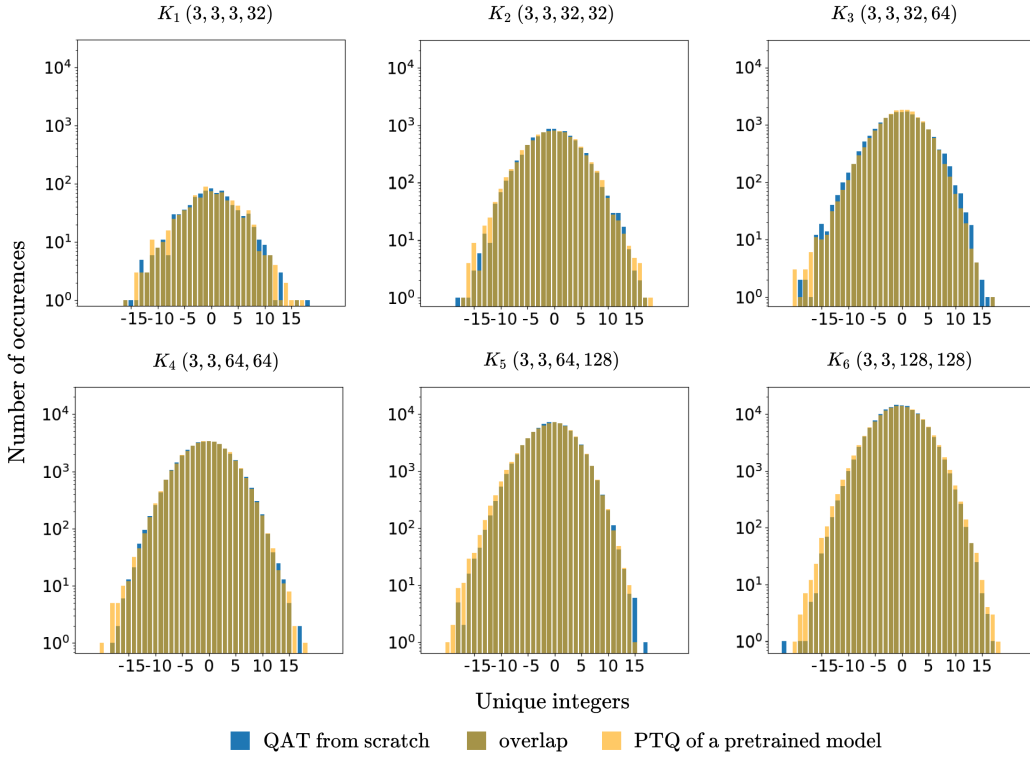


Figure 4.6: Quantization of CIFAR-10 kernels with row-wise granularity at $\lambda = 1e - 11$.

In PTQ, we achieve results similar to those observed in dense layers, as shown in Figure 4.5 and Figure 4.6. However, the validation loss progression during PTQ, demonstrated in Figure 4.8, shows an interesting pattern for $\lambda = 1e - 8$. We observe that the validation loss increases initially but decreases towards the end. This stabilization occurs when the model reaches a significant level of quantization — indicated by m (introduced in Subsection 3.1.2), the maximum integer value for a given scale factor, becoming very small. As m drops, the gradient updates for the corresponding scale factor also shrink, causing the scale factors to converge. Such convergence, in its turn, helps the pretrained model to re-stabilize. These observations suggest that the gradient-based approach may also be effective for PTQ scenarios where pretrained models need to be quantized.

Table 4.4: Compression rate of the nested quantization layer method

Dataset	Baseline	PTQ + Compression	Granularity, λ
MNIST	≈ 0.36 MB	≈ 0.05 MB	row-wise, $1e - 10$
CIFAR-10	≈ 1.02 MB	≈ 0.16 MB	row-wise, $1e - 11$
Imagenette	≈ 39.57 MB	≈ 6.39 MB	channel-wise, $1e - 11$

4 Experiments

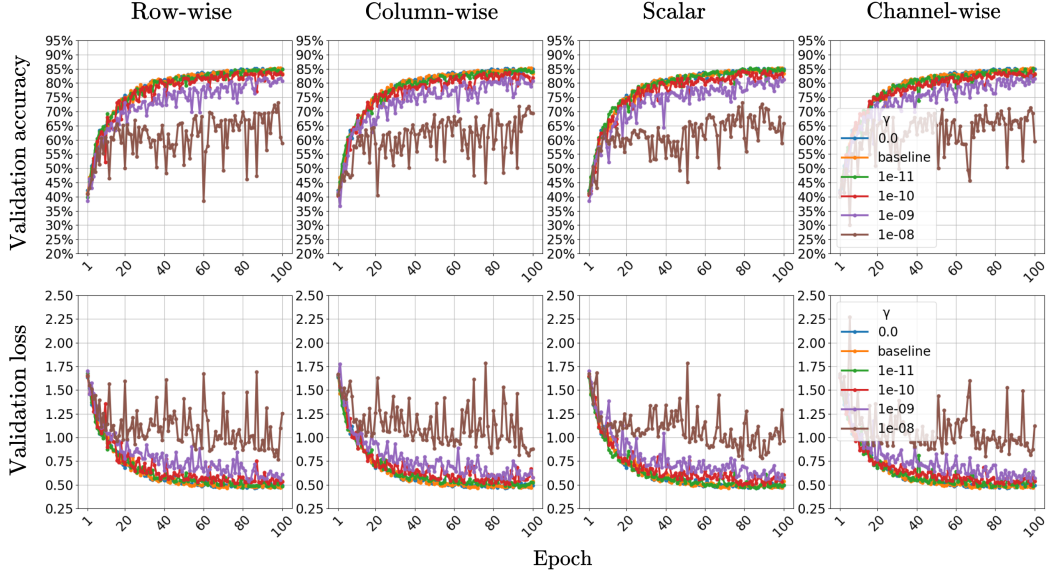


Figure 4.7: Impact of quantization on accuracy and loss for different λ on CIFAR-10.

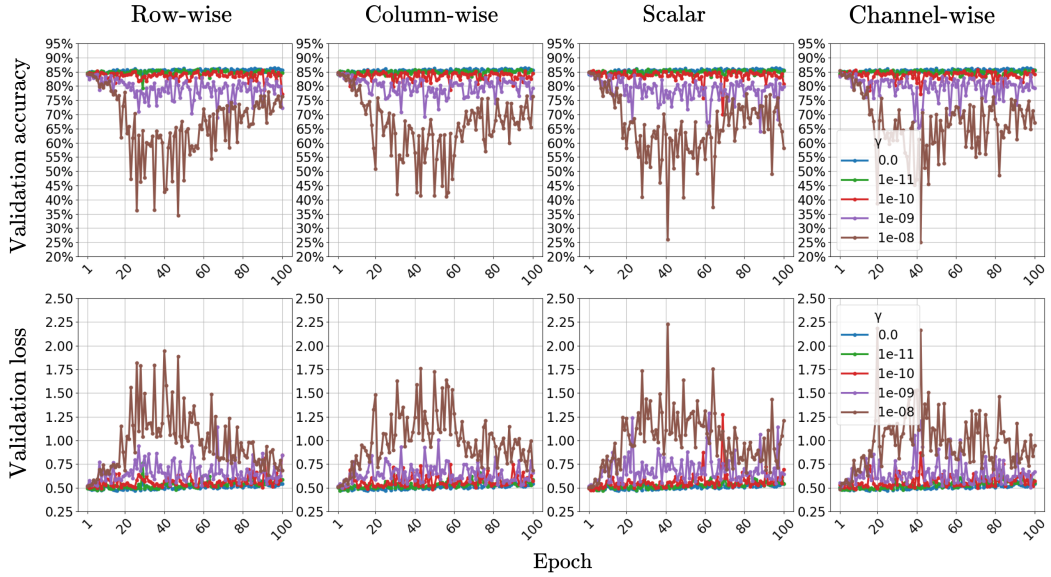


Figure 4.8: Impact of PTQ on accuracy and loss for different λ on CIFAR-10.

For the Imagenette dataset, we define a ResNet-inspired network with twenty convolutional layers. Similarly, we examine four scenarios, each corresponding to different granularities. While the specific kernel sizes differ, the logic for assigning scale factor configurations follows the same approach as outlined in Table 4.3.

4.2 Analysis of Nested Quantization Layers

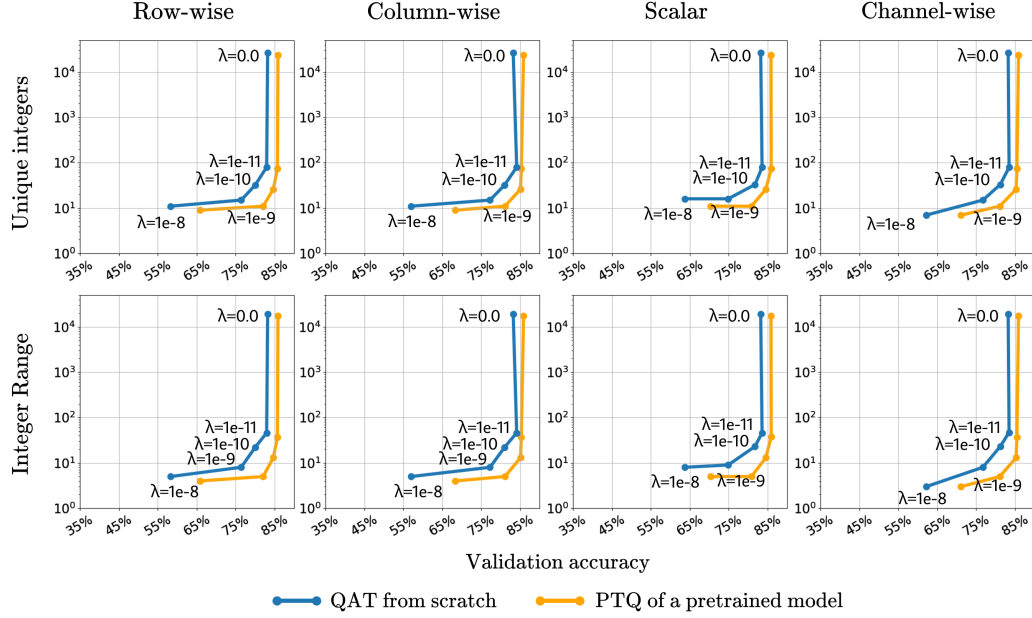


Figure 4.9: Accuracy–quantization trade-off for nested quantization layers on Imagenette.

The resulting Pareto front plots are depicted in Figure 4.9, where we see that PTQ has yielded significant accuracy improvement. This improvement is connected to the learning rate decay. Specifically, when we take a pretrained model that ended its training with a very low learning rate and begin retraining to quantize with a larger learning rate, the model essentially becomes more flexible, accommodating further convergence.

Similar to the observations on CIFAR-10, we do not see a significant difference between various granularity settings applied to Imagenette convolutional layers.

Table 4.4 presents the compressed file sizes of dense or convolutional layers before and after applying our PTQ in selected scenarios. To ensure a fair comparison, the Baseline column reflects the size of the original, unquantized FP32 weights and biases, which are compressed using zipping. The PTQ + Compressed column, on the other hand, shows the size after quantization and compression.

Specifically, the quantization and compression process involves flooring the weights and biases to INT8 format, saving them as `.npy` files, and subsequently compressing these files using zipping. It is important to note that this compression method is intended solely for demonstration purposes, to highlight the potential reduction gains, and does not necessarily represent an efficient deployment format.

Across the three datasets, we observe up to an eight-fold reduction in file size. We also note that the scaling factors must be saved separately in FP32, since they are used during the forward-pass to rescale the weights and biases. However, these full-precision scale factors are relatively small, so their storage overhead is minimal.

4 Experiments

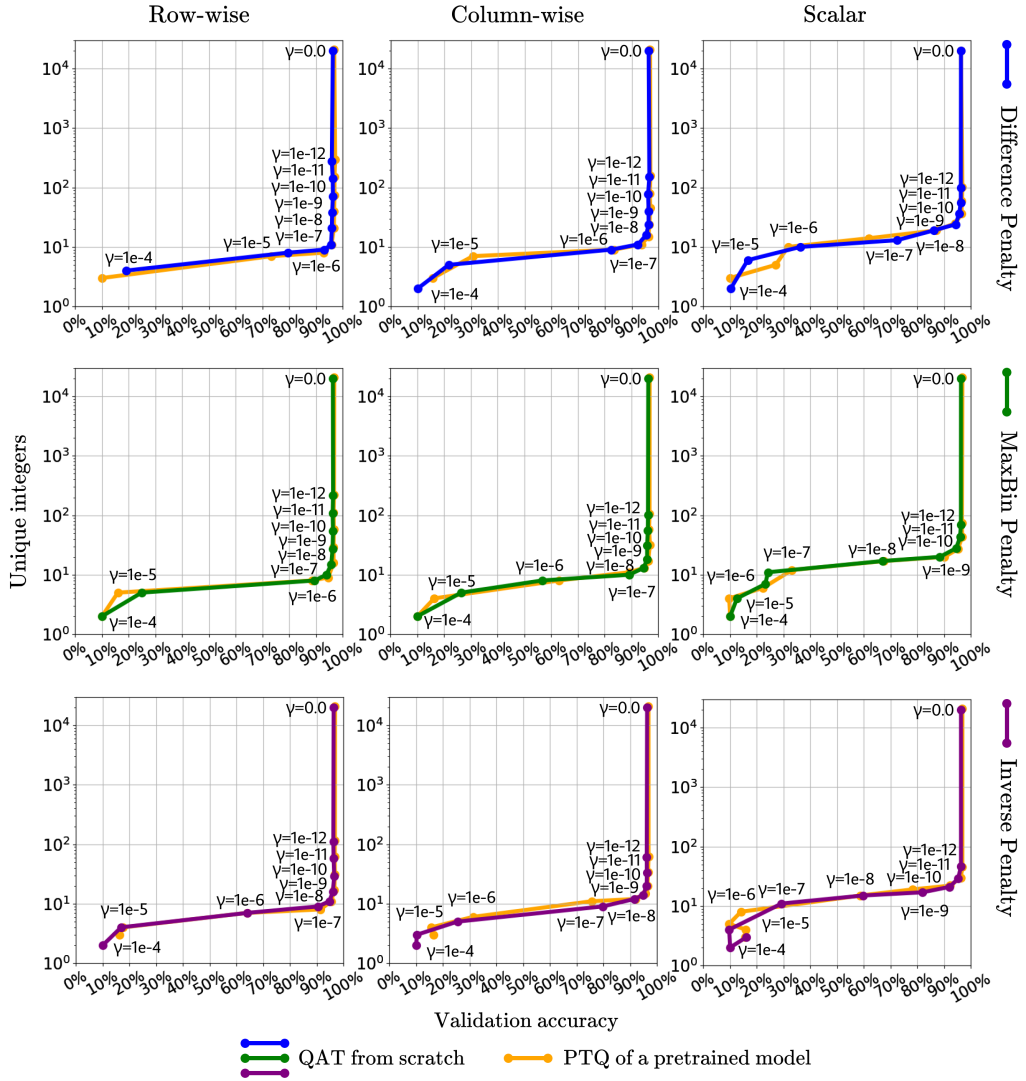


Figure 4.10: Accuracy–quantization trade-off for custom loss terms on MNIST.

4.3 Analysis of Custom Loss Terms

For the custom loss term methods, we examine their behavior under different penalty rates γ for the same three models discussed earlier, following a similar approach to the previous section.

4.3.1 Fully Connected Layers

We compare the three custom loss function terms applied to the two dense layers of the model trained on MNIST. The resulting Pareto front plots are shown in Figure 4.10. We

4.3 Analysis of Custom Loss Terms

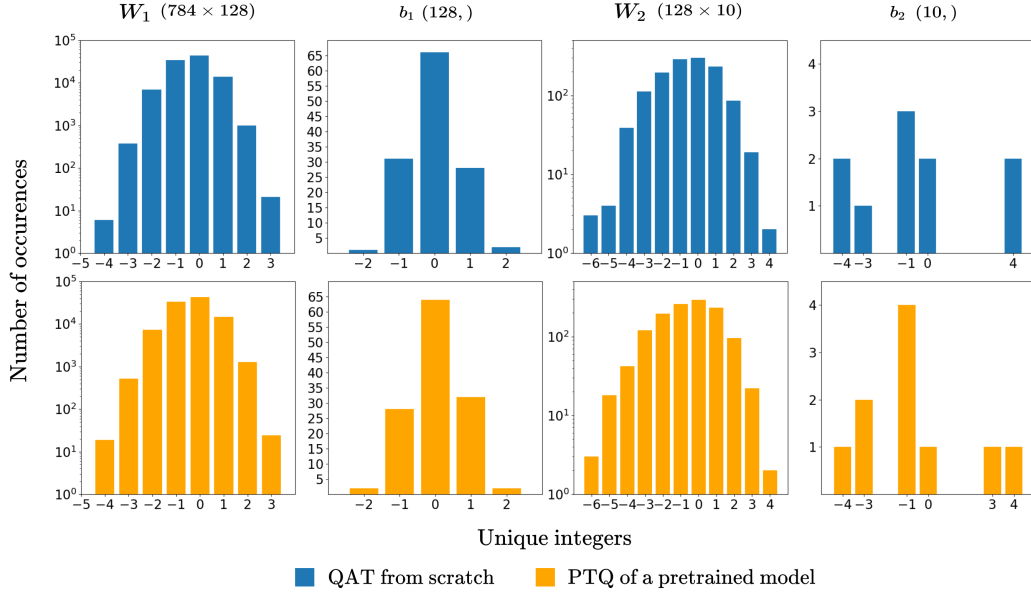


Figure 4.11: Quantization of MNIST dense layers with row-wise granularity at $\gamma = 1e-7$ with Difference Penalty.

can conclude that the row-wise scenario with the Difference Penalty is the optimal one as its Pareto front forms the sharpest angle, the vertex of which is closest to the lower right corner of the plot, indicating an optimal balance between the number of unique integers and validation accuracy. This vertex corresponds to $\gamma = 1e-7$, that results in integers from -6 to 2 , requiring only 4 bits, as demonstrated in Figure 4.11.

The optimality of the row-wise Difference Penalty case is further supported by Figure 4.12, where the validation loss for this scenario starts increasing only at $\gamma = 1e-6$, while the other granularity and custom loss term combinations experience a significantly greater increase in loss at the same value of γ .

From Figure 4.12, we can make the following additional observations. First, scalar granularity is the most aggressive among the three granularities, resulting in the poorest performance due to its excessive coarseness. Second, the Inverse Penalty stands out as the most aggressive custom loss term, which is intuitive, as the scale factors are initialized with very small values, leading to larger gradient updates proportional to the inverse of these factors. Consequently, the combination of scalar granularity and the Inverse Penalty performs the worst among all combinations, although it still achieves reasonably good quantization, with fewer than 100 unique integers for $\gamma = 1e-12$.

In terms of PTQ, we observe results approximately similar to those of QAT from scratch, as shown in Figure 4.10 and Figure 4.11. The progression of validation loss for each scenario follows the same pattern as in Figure 4.12, although the initial value at the start of training is closer to 0.25 due to the use of a pretrained model.

4 Experiments

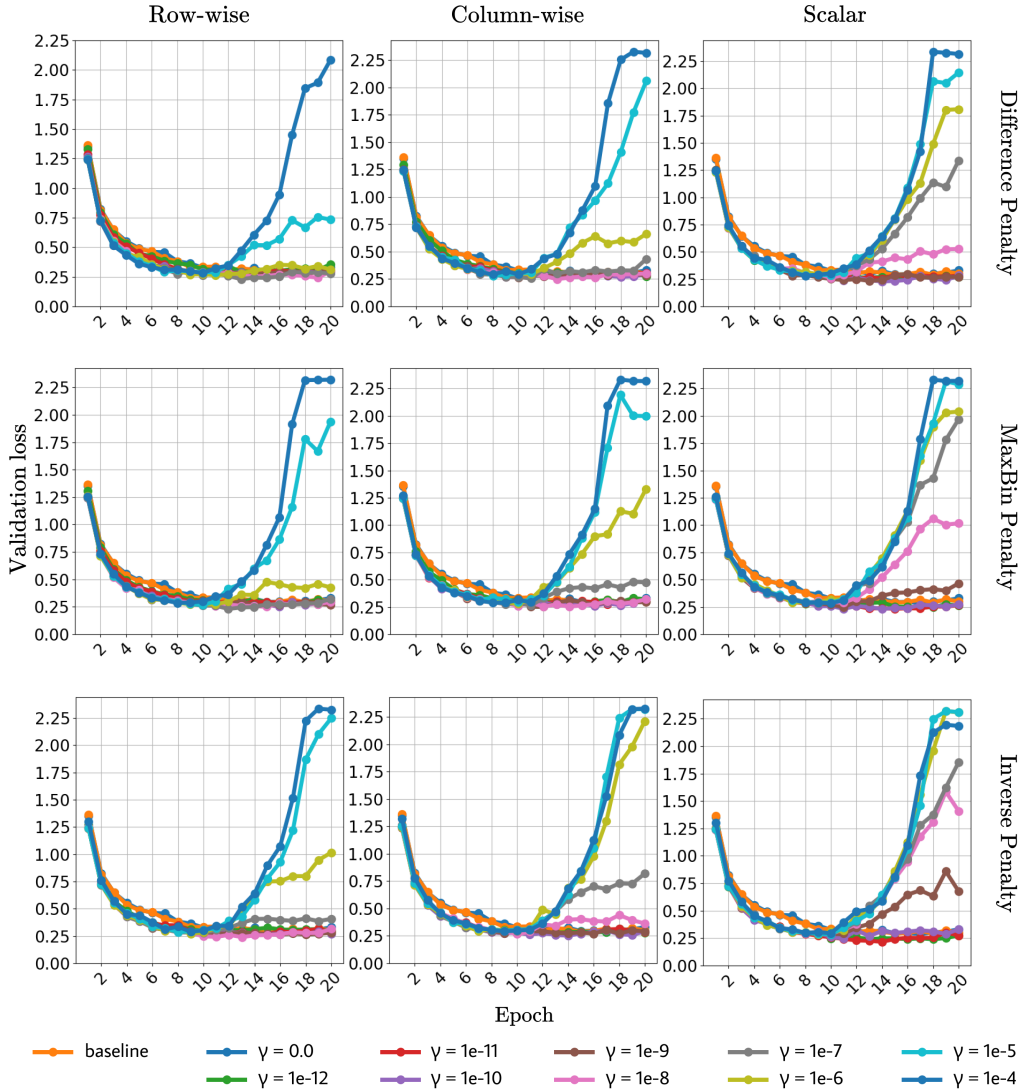


Figure 4.12: Impact of quantization on accuracy and loss for different γ on MNIST.

4.3.2 Convolutional Layers

We now compare the loss function terms applied to the convolutional layers of the model trained on CIFAR-10. Based on the results summarized in Figure 4.13 and Figure 4.14, the conclusion that the scalar granularity combined with the Inverse Penalty approach is the most aggressive remains valid. However, we observe that the channel-wise granularity is the most suitable configuration in this case, with $\gamma = 1e-10$ producing integers ranging from -28 to 34 in the kernels of the convolutional layers. These integers form a bell curve closely resembling the experimental results of the nested quantization

4.3 Analysis of Custom Loss Terms

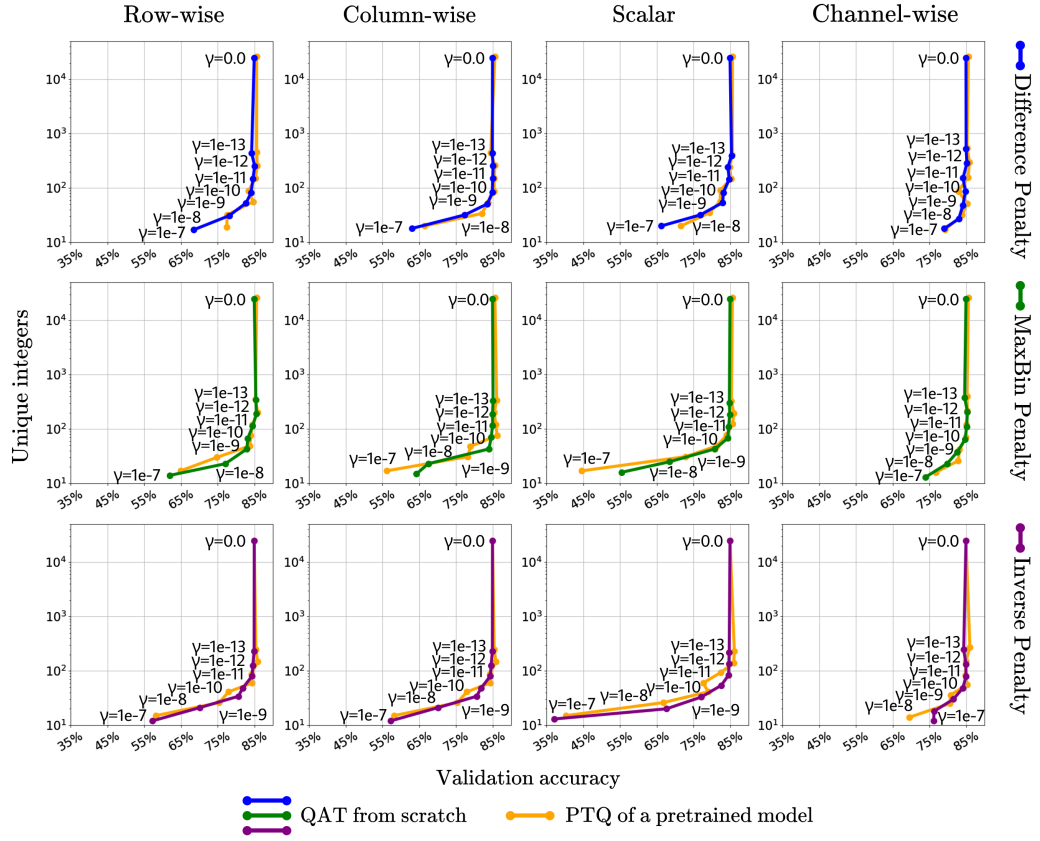


Figure 4.13: Accuracy – Quantization Trade-off for Custom Loss Terms on CIFAR-10.

layer with rowwise granularity for $\lambda = 1e - 11$ depicted in Figure 4.6 It is worth noting that, compared to the gradient-based nested quantization layer approach, the custom loss terms lead to more outliers in the resulting integers of biases. This behavior can be attributed to the custom loss term formulations, specifically how they are scaled with the number of parameters in each kernel and bias. Since the bias scale factors affect significantly fewer individual parameters than the kernels, their contribution to the loss term is smaller, leading to much smaller updates.

Similar to the other experiments, we conduct PTQ using a full-precision pretrained model. The results of PTQ are closely comparable to those obtained through QAT as evident from Figure 4.13 — which demonstrates the effectiveness of learned quantization in achieving similar outcomes without the need for a separate pretraining phase. Furthermore, the PTQ results for the channel-wise granularity and Difference Penalty combination we highlighted earlier align closely with those observed in the learned quantization scenario.

For the model trained on Imagenette, the custom loss terms fail to form a Pareto front as depicted in Figure 4.15, although reasonable quantization is achieved with minimal

4 Experiments

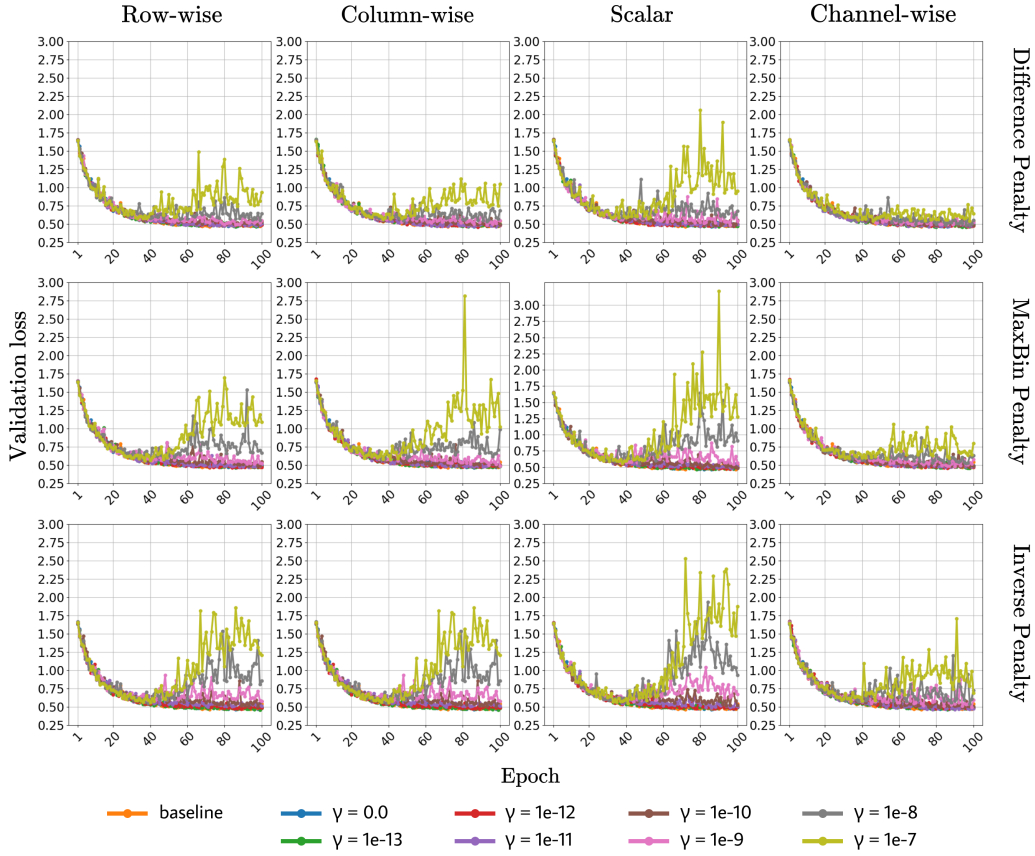


Figure 4.14: Impact of quantization on accuracy and for different γ and custom loss function terms on CIFAR-10.

accuracy loss. This behavior is attributed to the learning rate decay, which prevents the model from reaching a quantization level that could significantly impact accuracy once the learning rate becomes too small. In contrast, the nested quantization layer approach quantizes more rapidly, ultimately "breaking" the model for larger values of the corresponding hyperparameter before the learning rate decay limits further updates.

Nevertheless, for the Imagenette dataset, we observe improved accuracy in the PTQ scenario as noticed in the case with the nested quantization layer.

Table 4.5 presents the file sizes of dense or convolutional layers before and after applying our PTQ in selected training scenarios. For demonstration purposes, we use the same compression technique as in the nested quantization layer approach. Across all datasets, we observe a substantial reduction in file size, with reductions sometimes exceeding a factor of 10.

4.3 Analysis of Custom Loss Terms

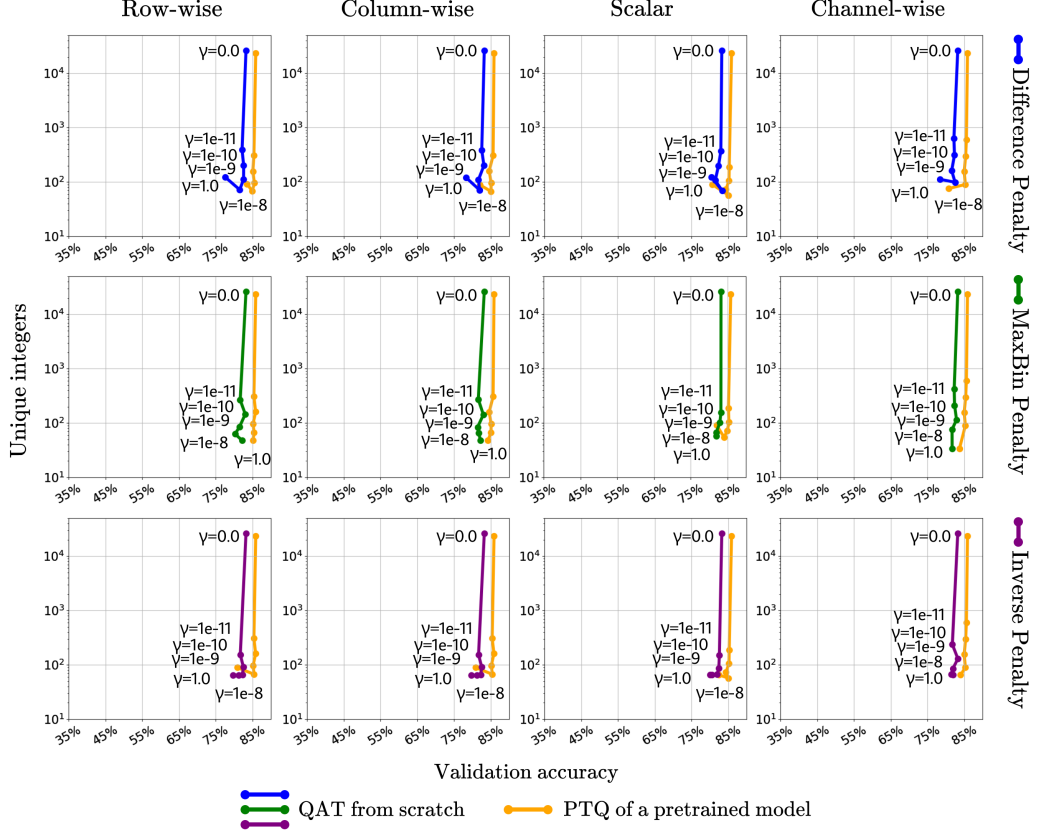


Figure 4.15: Accuracy – Quantization Trade-off for Custom Loss Terms on Imagenette.

Table 4.5: Compression rate for chosen quantization scenarios

Combination	Baseline	PTQ + Compression	Granularity, γ
MNIST, Difference	≈ 0.36 MB	≈ 0.03 MB	row-wise, $1e-7$
MNIST, MaxBin	≈ 0.36 MB	≈ 0.04 MB	row-wise, $1e-8$
MNIST, Inverse	≈ 0.36 MB	≈ 0.04 MB	row-wise, $1e-9$
CIFAR-10, Difference	≈ 1.02 MB	≈ 0.17 MB	channel-wise, $1e-10$
CIFAR-10, MaxBin	≈ 1.02 MB	≈ 0.15 MB	channel-wise, $1e-10$
CIFAR-10, Inverse	≈ 1.02 MB	≈ 0.16 MB	channel-wise, $1e-11$
Imagenette, Difference	≈ 39.57 MB	≈ 5.90 MB	channel-wise, $1e-9$
Imagenette, MaxBin	≈ 39.57 MB	≈ 6.46 MB	channel-wise, $1e-9$
Imagenette, Inverse	≈ 39.57 MB	≈ 5.37 MB	channel-wise, $1e-8$

4 Experiments

5 Related Work

The hyperparameter space of deep neural networks is so vast that classifying research in the field of learned quantization into rigid groups is inherently challenging. Nevertheless, we aim to outline a rough distinction between different approaches by emphasizing their most apparent aspects, after first establishing the position of learned quantization within the broader field of quantization.

Data-Free vs. Data-Driven Quantization. As discussed in Chapter 2, data-free quantization relies solely on the intrinsic properties of ML models, such as weight distribution statistics, to determine quantization parameters [33]. In contrast, data-driven quantization uses the original training data to fine-tune the model to the quantization strategy [46]. Although learned quantization does not strictly align with the definition of a fine-tuning process, it incorporates the full training pipeline, jointly optimizing both the model and the quantization parameters. This characteristic makes it inherently data-driven. Thus, we regard learned quantization as a distinct subcategory within data-driven quantization approaches.

PTQ vs. QAT. Although PTQ and QAT are often presented as contrasting approaches in the literature, they differ fundamentally in their nature. PTQ refers to a collection of techniques applied after a model has been trained to quantize its parameters, whereas QAT is a specific training process where the model is trained while incorporating quantization constraints throughout the training phase. Thus, we classify QAT as part of learned quantization, while PTQ is considered a distinct approach, situated between data-free and data-driven quantization methods, as PTQ [50] can fall into either category depending on the parameters being quantized. When only weights are quantized, the process is data-free, as weights can be quantized without relying on input data. When activations are included, the process becomes data-driven, since activation quantization requires input data for calibration.

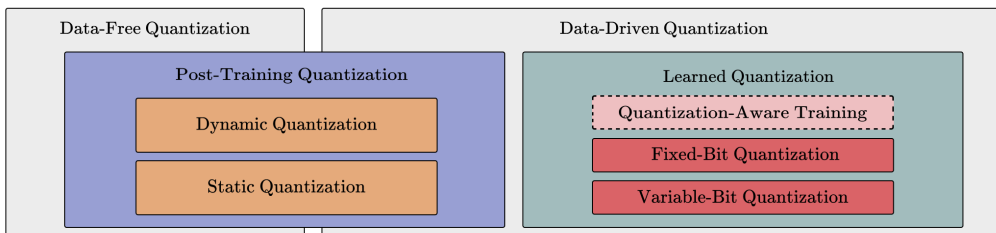


Figure 5.1: Learned quantization in a broad context.

5 Related Work

Static vs. Dynamic Quantization. Static quantization is an offline method that quantizes weights and activations before inference, whereas dynamic quantization is applied on-the-fly during inference. Both static and dynamic quantization methods are post-training approaches. In the context of learned quantization, static quantization might refer to a fixed quantization scheme, and dynamic quantization — to a scheme that depends on trainable quantizers. However, these terms are not commonly used this way in the literature. Therefore, we consider static and dynamic quantization separately from learned quantization.

Having established the broader context of quantization, we will now attempt to classify the various approaches within learned quantization itself.

Fixed-Bit vs. Variable-Bit. Learned quantization schemes can be roughly divided into two broader groups. The first group involves quantization schemes that use a fixed target bit size, while the second group aims to learn or effectively determine the lowest feasible bit size. This distinction is not widely discussed in the literature, but we view it as a recognizable pattern. For example, LQ-Nets [47] compute binary encodings of model parameters using a predefined bit size, whereas LSQ [11] learns step sizes in a way that can adaptively reduce bit-width requirements.

Quantization Target. NNs offer multiple opportunities for applying quantization. While some learned quantization approaches focus exclusively on model weights [7, 10, 36, 38], others extend the target to include activations [19, 25, 39, 46, 47] and even gradients [31, 48]. As notable examples, DoReFa-Net [49] quantizes all three with arbitrary bit widths, whereas Quantized Neural Networks [19] constrain weights and activations to either -1 or $+1$, and quantize gradients to 6 bits.

Quantization Precision. The target lower bit precision, and whether it is adjustable, varies between methods — ranging from rigid constraints to only a few values, to the flexibility of setting the desired bit width. For instance, BinaryNet [18] and XNOR-Net [39] represent extreme cases of quantization, where weights and activations are binarized. Ternary Weight Networks [32] take a slightly less aggressive approach by quantizing weights to $-1, 0, 1$. In contrast, DoReFa-Net [49] allows the target bit size to be defined. We note that this classification represents a subset of fixed-bit quantization methods, where the target precision is predefined and does not adapt during training.

Quantization Granularity. Learned quantization methods differ in how granularly the quantization is applied, that is, the level of detail at which model parameters are quantized. To illustrate, Benoit et al. [21] implement layer-wise quantization — similar to QIL [23] and PACT [5] — whereas LQ-Nets [47] employ channel-wise quantization for weights, despite using layer-wise quantization for activations.

Combination with Other Techniques. A number of learned quantization methods work in unison with other model compression approaches. For example, Deep Compression [15] combines quantization with pruning, while Polino et al. [38] and Wei et al. [43] jointly leverage quantization and knowledge distillation.

Within the above classifications, our proposed method falls under fixed-bit quantization, unless the resulting integer values are further compressed to lower bit widths based on their range. Our methods address both weight and bias quantization, though

bias quantization is relatively uncommon due to the typically small size of bias vectors. Additionally, the methods incorporate varying granularities for applying scaling factors.

While not directly integrated with other techniques, it is worth noting that learned sparsification methods, such as DeepHoyer [45], share similarities with our custom loss term approach. Specifically, both employ differentiable loss terms to achieve a structural property — sparsification in the case of DeepHoyer and quantization in our work.

Our gradient-based nested quantization layer is distinct in that it uses a controllable hyperparameter and utilizes the gradients of the parameters to be quantized to calculate updates for the scale factors. Conceptually, this approach takes a "look from within" — unlike most methods, which focus on designing or approximating differentiable forward-pass operations for quantization, we shift the focus to modifying the back-propagation, a less common approach to incorporating quantization logic.

5 Related Work

6 Conclusions

In this thesis, we propose two methods that revolve around making ML models learn scale factors to achieve quantization of adjustable intensity. In the first approach, we introduce a nested quantization layer — one that updates its scale factors through a threshold-based gradient logic. Only parameters deemed *non-sensitive* contribute to the decision of whether coarser quantization should be pursued. In the second approach, scale factor updates come from custom loss terms — MaxBin, Inverse, and Difference — each employing distinct logic to guide quantization intensity through a penalty rate.

Our experiments demonstrate that the nested quantization layer approach achieves compression rates of up to $8\times$ on the MNIST dataset, and around $6\times$ on CIFAR-10 and Imagenette, with minimal accuracy degradation. The optimal penalty threshold was $\lambda = 1e-10$ for the MNIST model (where dense layers were quantized), and $\lambda = 1e-11$ for CIFAR-10 and Imagenette (where convolutional layers were quantized). Interestingly, for the MNIST dataset, the added noise from quantization appeared to improve model confidence, as evidenced by a lower validation loss relative to the baseline.

Regarding the custom loss terms, they yield compression rates of up to $10\times$ or more. On MNIST and CIFAR-10, the Difference penalty provided the best results — using row-wise granularity in MNIST and channel-wise granularity in CIFAR-10. By contrast, on Imagenette, all custom loss terms behaved similarly due to the learning-rate configuration for that model. Notably, our post-training quantization-aware training — as we put it — resulted in a significant accuracy improvement for Imagenette, while yielding performance comparable to the from-scratch quantization scenarios on MNIST and CIFAR-10.

There remains significant room for further exploration, especially in extending experiments to scenarios where both dense and convolutional layers are quantized simultaneously. This could involve employing different penalty thresholds or penalty rates for individual layers. Another valid direction would be testing the proposed methods on established architectures such as AlexNet. While the nested quantization layer takes parameter sensitivity into account, introducing adjustments based on layer-wide sensitivity would be logical — as widely argued in the literature, not all layers respond equally to quantization. For instance, first and last layers are often left in full precision.

We acknowledge that the custom methods introduced in this work add complexity, as they require additional computations. Moreover, in real-world scenarios, tracking the progression of quantization is difficult for large models — a disadvantage that cannot be ignored when adjusting the intensity of the penalty threshold or rate.

Given the limits of the current methods, future work should focus on improving these methods further while focusing on the theoretical aspect, instead of largely relying on experiments. Such a shift in focus means clearly defining the optimization problem and proving it can work in theory by providing a rigorous algorithmic solution.

6 Conclusions

Nevertheless, our proposed methods are, if not the first, then among the earliest to employ a nested logic — a quantization layer that is called within a standard layer. The threshold-based gradient method also presents itself as a rather novel approach, taking an alternative direction¹ by focusing on gradient manipulation directly.

Bibliography

- [1] Dorra Ben Khalifa and Matthieu Martel. “Rigorous Floating-Point to Fixed-Point Quantization of Deep Neural Networks on STM32 Micro-controllers”. In: *CoDIT*. IEEE, 2024, pp. 1201–1206. DOI: [10.1109/CoDIT62066.2024.10708400](https://doi.org/10.1109/CoDIT62066.2024.10708400). URL: <https://doi.org/10.1109/CoDIT62066.2024.10708400>.
- [2] Yoshua Bengio, Nicholas Léonard, and Aaron C. Courville. “Estimating or Propagating Gradients Through Stochastic Neurons for Conditional Computation”. In: *CoRR* abs/1308.3432 (2013). arXiv: 1308.3432. URL: <http://arxiv.org/abs/1308.3432>.
- [3] Tom B. Brown et al. “Language Models are Few-Shot Learners”. In: *NeurIPS*. 2020. URL: <https://arxiv.org/abs/2005.14165>.
- [4] Jun Chen et al. “Propagating Asymptotic-Estimated Gradients for Low Bitwidth Quantized Neural Networks”. In: *IEEE Journal of Selected Topics in Signal Processing* 14.4 (2020), pp. 848–859. DOI: [10.1109/JSTSP.2020.2966327](https://doi.org/10.1109/JSTSP.2020.2966327). URL: <https://doi.org/10.1109/JSTSP.2020.2966327>.
- [5] Jungwook Choi et al. “PACT: Parameterized Clipping Activation for Quantized Neural Networks”. In: *CoRR* abs/1805.06085 (2018). arXiv: 1805.06085. URL: <http://arxiv.org/abs/1805.06085>.
- [6] Yoojin Choi, Mostafa El-Khamy, and Jungwon Lee. “Learning Sparse Low-Precision Neural Networks With Learnable Regularization”. In: *IEEE Access* 8 (2020), pp. 96963–96974. DOI: [10.1109/ACCESS.2020.2996936](https://doi.org/10.1109/ACCESS.2020.2996936). URL: <https://doi.org/10.1109/ACCESS.2020.2996936>.
- [7] Matthieu Courbariaux, Yoshua Bengio, and Jean-Pierre David. “BinaryConnect: Training Deep Neural Networks with binary weights during propagations”. In: *NeurIPS*. 2015. URL: <https://proceedings.neurips.cc/paper/2015/hash/3e15cc11f979ed25912dff5b0669f2cd-Abstract.html>.
- [8] Ahmed T. Elthakeb, Prannoy Pilligundla, and Hadi Esmaeilzadeh. “SinReQ: Generalized Sinusoidal Regularization for Automatic Low-Bitwidth Deep Quantized Training”. In: *CoRR* abs/1905.01416 (2019). arXiv: 1905.01416. URL: <http://arxiv.org/abs/1905.01416>.
- [9] Ahmed T. Elthakeb et al. “Gradient-Based Deep Quantization of Neural Networks through Sinusoidal Adaptive Regularization”. In: *CoRR* abs/2003.00146 (2020). arXiv: 2003.00146. URL: <https://arxiv.org/abs/2003.00146>.

Bibliography

- [10] Steven K. Esser et al. “Convolutional networks for fast, energy-efficient neuromorphic computing”. In: *PNAS* 113.41 (2016), pp. 11441–11446. DOI: 10.1073/PNAS.1604850113. URL: <https://doi.org/10.1073/pnas.1604850113>.
- [11] Steven K. Esser et al. “Learned Step Size quantization”. In: *ICLR*. 2020. URL: <https://openreview.net/forum?id=rkg066VKDS>.
- [12] Amir Gholami et al. “A Survey of Quantization Methods for Efficient Neural Network Inference”. In: *CoRR* abs/2103.13630 (2021). arXiv: 2103.13630. URL: <https://arxiv.org/abs/2103.13630>.
- [13] Robert M. Gray and David L. Neuhoff. “Quantization”. In: *IEEE Trans. Inf. Theory* 44.6 (1998), pp. 2325–2383. DOI: 10.1109/18.720541. URL: <https://doi.org/10.1109/18.720541>.
- [14] Philipp Gysel et al. “Ristretto: A Framework for Empirical Study of Resource-Efficient Inference in Convolutional Neural Networks”. In: *IEEE Transactions on Neural Networks and Learning Systems* 29.11 (2018), pp. 5784–5789. DOI: 10.1109/TNNLS.2018.2808319. URL: <https://doi.org/10.1109/TNNLS.2018.2808319>.
- [15] Song Han, Huizi Mao, and William J. Dally. “Deep Compression: Compressing Deep Neural Network with Pruning, Trained Quantization and Huffman Coding”. In: *ICLR*. Ed. by Yoshua Bengio and Yann LeCun. 2016. URL: <http://arxiv.org/abs/1510.00149>.
- [16] Jeremy Howard and Sylvain Gugger. “Fastai: A Layered API for Deep Learning”. In: *Information* 11.2 (2020), p. 108. DOI: 10.3390/INF011020108. URL: <https://doi.org/10.3390/info11020108>.
- [17] Gao Huang et al. “Densely Connected Convolutional Networks”. In: *CVPR*. 2017. DOI: 10.1109/CVPR.2017.243. URL: <https://doi.org/10.1109/CVPR.2017.243>.
- [18] Itay Hubara et al. “Binarized Neural Networks”. In: *NeurIPS*. 2016. URL: <https://dl.acm.org/doi/10.5555/3157382.3157557>.
- [19] Itay Hubara et al. “Quantized Neural Networks: Training Neural Networks with Low Precision Weights and Activations”. In: *JMLR* 18 (2017), 187:1–187:30. URL: <https://jmlr.org/papers/v18/16-456.html>.
- [20] David A. Huffman. “A Method for the Construction of Minimum-Redundancy Codes”. In: *Proceedings of the IRE* 40.9 (1952), pp. 1098–1101. DOI: 10.1109/JRPROC.1952.273898. URL: <https://ieeexplore.ieee.org/document/4051119>.
- [21] Benoit Jacob et al. “Quantization and Training of Neural Networks for Efficient Integer-Arithmetic-Only Inference”. In: *CVPR*. 2018. DOI: 10.1109/CVPR.2018.00286. URL: http://openaccess.thecvf.com/content_cvpr_2018/html/Jacob_Quantization_and_Training_CVPR_2018_paper.html.
- [22] Chutian Jiang. “Efficient Quantization Techniques for Deep Neural Networks”. In: *CONF-SPML*. 2021. DOI: 10.1109/CONF-SPML54095.2021.00059. URL: <https://doi.org/10.1109/CONF-SPML54095.2021.00059>.

Bibliography

- [23] Sangil Jung et al. “Learning to Quantize Deep Networks by Optimizing Quantization Intervals With Task Loss”. In: *CVPR*. 2019. DOI: 10.1109/CVPR.2019.00448. URL: http://openaccess.thecvf.com/content_CVPR_2019/html/Jung_Learning_to_Quantize_Deep_Networks_by_Optimizing_Quantization_Intervals_With_CVPR_2019_paper.html.
- [24] Daya Shanker Khudia et al. “FBGEMM: Enabling High-Performance Low-Precision Deep Learning Inference”. In: *CoRR* abs/2101.05615 (2021). arXiv: 2101.05615. URL: <https://arxiv.org/abs/2101.05615>.
- [25] Raghuraman Krishnamoorthi. “Quantizing deep convolutional networks for efficient inference: A whitepaper”. In: *CoRR* abs/1806.08342 (2018). arXiv: 1806.08342. URL: <http://arxiv.org/abs/1806.08342>.
- [26] Alex Krizhevsky. “Learning Multiple Layers of Features from Tiny Images”. In: *University of Toronto* (May 2012). URL: <https://www.cs.toronto.edu/~kriz/learning-features-2009-TR.pdf>.
- [27] Alex Krizhevsky, Ilya Sutskever, and Geoffrey E. Hinton. “ImageNet Classification with Deep Convolutional Neural Networks”. In: *NeurIPS*. 2012. URL: <https://proceedings.neurips.cc/paper/2012/hash/c399862d3b9d6b76c8436e924a68c45b-Abstract.html>.
- [28] Yann LeCun, Yoshua Bengio, and Geoffrey E. Hinton. “Deep learning”. In: *Nature* 521.7553 (2015), pp. 436–444. DOI: 10.1038/NATURE14539. URL: <https://doi.org/10.1038/nature14539>.
- [29] Yann LeCun, Corinna Cortes, and CJ Burges. “MNIST handwritten digit database”. In: *ATT Labs [Online]* 2 (2010). URL: <http://yann.lecun.com/exdb/mnist>.
- [30] Qun Li et al. “Investigating the Impact of Quantization on Adversarial Robustness”. In: *CoRR* abs/2404.05639 (2024). DOI: 10.48550/ARXIV.2404.05639. arXiv: 2404.05639. URL: <https://doi.org/10.48550/arXiv.2404.05639>.
- [31] Zhouhan Lin et al. “Neural Networks with Few Multiplications”. In: *ICLR*. Ed. by Yoshua Bengio and Yann LeCun. 2016. URL: <http://arxiv.org/abs/1510.03009>.
- [32] Bin Liu et al. “Ternary Weight Networks”. In: *IEEE-ICASSP*. 2023. DOI: 10.1109/ICASSP49357.2023.10094626. URL: <https://doi.org/10.1109/ICASSP49357.2023.10094626>.
- [33] Markus Nagel et al. “Data-Free Quantization Through Weight Equalization and Bias Correction”. In: *ICCV*. 2019. DOI: 10.1109/ICCV.2019.00141. URL: <https://doi.org/10.1109/ICCV.2019.00141>.
- [34] Maxim Naumov et al. “On Periodic Functions as Regularizers for Quantization of Neural Networks”. In: *CoRR* abs/1811.09862 (2018). arXiv: 1811.09862. URL: <http://arxiv.org/abs/1811.09862>.
- [35] Pierre-Emmanuel Novac et al. “Quantization and Deployment of Deep Neural Networks on Microcontrollers”. In: *CoRR* abs/2105.13331 (2021). arXiv: 2105.13331. URL: <https://arxiv.org/abs/2105.13331>.

Bibliography

- [36] Joachim Ott et al. “Recurrent Neural Networks With Limited Numerical Precision”. In: *CoRR* abs/1611.07065 (2016). arXiv: 1611.07065. URL: <http://arxiv.org/abs/1611.07065>.
- [37] Eunhyeok Park, Sungjoo Yoo, and Peter Vajda. “Value-Aware Quantization for Training and Inference of Neural Networks”. In: *ECCV*. 2018. DOI: 10.1007/978-3-030-01225-0__36. URL: https://doi.org/10.1007/978-3-030-01225-0\%5C_36.
- [38] Antonio Polino, Razvan Pascanu, and Dan Alistarh. “Model compression via distillation and quantization”. In: *ICLR*. 2018. URL: <https://openreview.net/forum?id=S1Xo1QbRW>.
- [39] Mohammad Rastegari et al. “XNOR-Net: ImageNet Classification Using Binary Convolutional Neural Networks”. In: *ECCV*. 2016. DOI: 10.1007/978-3-319-46493-0__32. URL: https://doi.org/10.1007/978-3-319-46493-0\%5C_32.
- [40] Álvaro Domingo Reguero, Silverio Martínez-Fernández, and Roberto Verdecchia. “Energy-efficient neural network training through runtime layer freezing, model quantization, and early stopping”. In: *Computer Standards & Interfaces* 92 (2025), p. 103906. DOI: 10.1016/J.CSI.2024.103906. URL: <https://doi.org/10.1016/j.csi.2024.103906>.
- [41] Pierre Stock et al. “Training with Quantization Noise for Extreme Model Compression”. In: *ICLR*. 2021. URL: <https://openreview.net/forum?id=dV19Yyi1fS3>.
- [42] Christian Szegedy et al. “Going deeper with convolutions”. In: *CVPR*. 2015. DOI: 10.1109/CVPR.2015.7298594. URL: <https://doi.org/10.1109/CVPR.2015.7298594>.
- [43] Yi Wei et al. “Quantization Mimic: Towards Very Tiny CNN for Object Detection”. In: *ECCV*. Ed. by Vittorio Ferrari et al. 2018. DOI: 10.1007/978-3-030-01237-3__17. URL: https://doi.org/10.1007/978-3-030-01237-3\%5C_17.
- [44] Carole-Jean Wu et al. “Sustainable AI: Environmental Implications, Challenges and Opportunities”. In: *CoRR* abs/2111.00364 (2021). arXiv: 2111.00364. URL: <https://arxiv.org/abs/2111.00364>.
- [45] Huanrui Yang, Wei Wen, and Hai Li. “DeepHoyer: Learning Sparser Neural Network with Differentiable Scale-Invariant Sparsity Measures”. In: *ICLR*. 2020. URL: <https://openreview.net/forum?id=ry1BK34FDS>.
- [46] Edouard Yvinec et al. “SPIQ: Data-Free Per-Channel Static Input Quantization”. In: *WACV*. 2023. DOI: 10.1109/WACV56688.2023.00386. URL: <https://doi.org/10.1109/WACV56688.2023.00386>.
- [47] Dongqing Zhang et al. “LQ-Nets: Learned Quantization for Highly Accurate and Compact Deep Neural Networks”. In: *ECCV*. Ed. by Vittorio Ferrari et al. 2018. DOI: 10.1007/978-3-030-01237-3__23. URL: https://doi.org/10.1007/978-3-030-01237-3\%5C_23.

Bibliography

- [48] Hantian Zhang et al. “ZipML: Training Linear Models with End-to-End Low Precision, and a Little Bit of Deep Learning”. In: *ICML*. 2017. URL: <http://proceedings.mlr.press/v70/zhang17e.html>.
- [49] Shuchang Zhou et al. “DoReFa-Net: Training Low Bitwidth Convolutional Neural Networks with Low Bitwidth Gradients”. In: *CoRR* abs/1606.06160 (2016). arXiv: 1606.06160. URL: <http://arxiv.org/abs/1606.06160>.
- [50] Xiaotian Zhu, Wengang Zhou, and Houqiang Li. “Adaptive Layerwise Quantization for Deep Neural Network Compression”. In: *ICME*. 2018. DOI: 10.1109/ICME.2018.8486500. URL: <https://doi.org/10.1109/ICME.2018.8486500>.